# Anchoring of nematic liquid crystals on mica in the presence of volatile molecules

B. Jérôme[1-3] and Y. R. Shen[1]

[1]*Department of Physics, University of California at Berkeley, Berkeley, California 94720*

[2]*Laboratoire de Physique des Solides, Bâtiment 510, Université de Paris–Sud, 91405 Orsay Cedex, France*

[3]*FOM—Institute for Atomic and Molecular Physics, Kruislaan 407, 1098 SJ Amsterdam, The Netherlands**

(Received 29 June 1993)

Using optical second-harmonic generation, we have studied the orientational order of cyanobiphenyl liquid-crystal monolayers at the interface between a mica crystal and a liquid-crystal film put in the presence of ethylene glycol vapor. These small, volatile molecules adsorb at the mica surface and significantly affect the orientational order of the surface liquid-crystal molecules. As the chemical potential of the volatile molecules was increased, this orientational order first varied continuously, and at a certain stage, exhibited a discontinuous change corresponding to a first-order orientational transition. This surface transition drives the first-order anchoring transition (i.e., the reorientation of the bulk liquid crystal) previously observed in these systems.

PACS number(s): 68.45.−v, 64.70.−p, 61.30.−v, 42.65.Ky

## I. INTRODUCTION

The phenomenon of orientation—or anchoring—of liquid crystals by surfaces has been known nearly as long as have liquid crystals themselves. During all these years and in particular in the past decade, numerous studies have been dedicated to this phenomenon; nevertheless, the mechanisms by which a surface can impose the orientation of a liquid-crystalline phase are far from being understood [1]. Most of the research in this field is done with nematic liquid crystals, which have the simplest known liquid-crystalline structure: the elongated molecules forming the liquid crystal orient on average parallel to each other. Anchoring of a nematic phase at a surface fixes the mean orientation taken by the molecules with respect to this surface. The chosen orientation is called the anchoring direction of the liquid crystal at the substrate surface.

Much of the progress made in the field in recent years has been due to techniques, such as second-harmonic-generation measurements [2] and scanning tunneling microscopy [3], which allow one to observe the microscopic behavior of liquid-crystal molecules at the surface of different substrates. It has in particular been shown that, in the case of nematic liquid crystals, one can distinguish two classes of alignment mechanisms [4,5]. The first ones are based on interactions between the liquid-crystal molecules and the substrate. These interactions determine the orientational order of the molecules in the first monolayer in contact with the substrate; this monolayer in turn orients the rest of the nematic phase via the intermolecular interactions which tend to align the molecules parallel to each other. One can in fact consider the bulk liquid crystal to be epitaxially grown on top of the surface monolayer [5,6]. In mechanisms of the second class, the director field adapts itself to the geometry of the substrate surface in order to minimize the elastic energy arising from distortions of this field. These mechanisms play a role in the case of nonflat surfaces such as grooved substrates.

A new challenge appeared a few years ago with the reports of several systems exhibiting anchoring transitions [1,7], i.e., systems in which the induced anchoring directions can be changed by varying system parameters [8–19]. Besides the fact that such transitions can be used to build new kinds of liquid-crystal displays driven by surface effects [15], understanding anchoring transitions should lead to a better understanding of the phenomenon of anchoring itself. Moreover, when these transitions are due to orientational transitions in the monolayer in contact with the substrate surface, they are an example of surface phase transitions driving macroscopic transitions [20].

Several anchoring transitions have been observed at the surface of cleaved muscovite mica crystals when water and/or alcohol molecules are added to the atmosphere surrounding the mica–liquid-crystal system [12,13]. These transitions involve a change in the orientation of the nematic phase in the plane of the substrate, which can be continuous (second-order transition) or discontinuous (first-order transition). This phenomenon has been attributed to the adsorption of volatile molecules (water and alcohol) at the mica surface, hence their name of "adsorption-induced" anchoring transitions [12]. Such an adsorption modifies the interface between the substrate and the liquid crystal, which can indeed induce changes in the anchoring directions taken by the nematic phase.

Following this idea, a phenomenological theory has been developed which qualitatively accounts for all the transitions which have been observed [12,13,21]. This theory considers the energy $\gamma$ of the interface between the substrate surface and the nematic phase. This interface is the transition region close to the surface in which

*Present address.

 

the nematic order is perturbed [1]. Since this interface is in equilibrium with a reservoir (the atmosphere) with constant temperature $T$ and constant chemical potential $\mu_i$ of volatile species, $\gamma$ is the grand potential $\Xi(T,\mu_i,\mathbf{n})$ of the interface, which depends on the orientation $\mathbf{n}$ of the nematic phase and is minimum when $\mathbf{n}$ is along an anchoring direction induced by the substrate. This theory shows that the density $\rho_i$ of volatile molecules at the interface is coupled to the orientation of the nematic phase since $\rho_i = -(\partial\Xi/\partial\mu_i)_{\mathbf{n},T}$. Thus first-order anchoring transitions (i.e., discontinuous changes in anchoring directions) should be associated with a jump in $\rho_i$. Using a simple model of nematic liquid crystal, Teixeira and Sluckin [22] have also shown that anchoring transitions (in their case involving changes in the tilt of the liquid-crystal axis with respect to the substrate surface) could be obtained when a nonmesogenic solute (i.e., a compound exhibiting no liquid-crystalline phases) is mixed to the liquid crystal and wets the substrate surface. Since none of these theories consider the detailed structure of the interface, they do not give any indication about the microscopic mechanisms leading to the observed anchoring transitions.

Since cleaved mica exhibits atomically smooth surfaces, the alignment of liquid crystals by these substrates must result from a mechanism belonging to the first class described above: the orientation of the bulk liquid crystal is due to the orientational order of the first monolayer of molecules in contact with the substrate surface. Information about the microscopic mechanisms inducing the anchoring transitions observed on mica should then be found in the behavior of the nematic molecules located at the substrate surface. Therefore we have performed second-harmonic-generation measurements on monolayers of cyanobiphenyl molecules at the surface of muscovite mica in the presence of ethylene glycol ($HOCH_2CH_2OH$) vapor. The principle of the technique and the experimental procedure are described in Sec. II and the results of the measurements are given in Sec. III. These measurements have allowed us to determine the orientational distribution of nematic molecules at the mica surface together with variations in their density (Sec. IV). We have observed that the adsorption of ethylene glycol molecules at the mica surface affects the orientational order of the liquid-crystal molecules at the mica surface; in particular, the surface monolayer exhibits a first-order orientational transition that can drive a bulk anchoring transition [20]. A possible mechanism leading to the observed surface transition is given, based on the molecular configuration of ethylene glycol molecules at the mica surface (Sec. V).

## II. EXPERIMENTAL PROCEDURE

### A. Second-harmonic-generation technique

The theory of second-harmonic generation by adsorbed species at substrate surfaces and its application to the determination of the orientational distribution in liquid-crystal monolayers have already been described in detail elsewhere [2,5,23]. We shall only recall here the essential elements for the understanding of the present article.

Let us consider a light beam at frequency $\omega$ incident on a mica surface covered with a few layers of liquid-crystal molecules such a cyanobiphenyl molecules ($NC\Phi\Phi C_nH_{2n+1}$ or $NC\Phi\Phi OC_nH_{2n+1}$), whose cyanobiphenyl rigid core exhibits a strong nonlinear polarizability. If the incident beam is sufficiently intense, the system has, in addition to its linear response, a nonlinear response whose first term generates light at frequency $2\omega$. Because of the boundary condition requiring the wave-vector components parallel to the surface to be matched [2], the second-harmonic signal must be coherently generated in the direction of reflection of the incident beam (Fig. 1).

The most important contribution to the reflected second-harmonic signal comes from the induced surface electric dipole polarization $\mathbf{P}_D^{(2)}(2\omega)=\bar{\chi}^D:\mathbf{E}(\omega)\mathbf{E}(\omega)$, where $\mathbf{E}(\omega)$ is the incident field at frequency $\omega$ and $\bar{\chi}^D$ is an effective surface nonlinear dipolar susceptibility of the illuminated medium. The bulk contribution to $\bar{\chi}^D$ vanishes in a centrosymmetric medium. This is the case for mica which has a $C_{2h}^6$ symmetry [24], as well as for the liquid crystal aside from the monolayer in contact with the mica surface. Indeed, away from the surface, cyanobiphenyl molecules form pairs of antiparallel molecules [25] and thus exhibit a quadrupolar ordering (Fig. 1).

The electric quadrupole nonlinearities of the mica and the liquid crystal also contribute to the second-harmonic generation but to a much lesser extent. For the liquid crystal, the induced nonlinear electric quadrupole polarization is $\mathbf{P}_Q^{(2)}(2\omega)=\bar{\chi}^Q:\mathbf{E}(\omega)\nabla\mathbf{E}(\omega)$ where $\bar{\chi}^Q$ is the nonlinear quadrupolar susceptibility of the material [26]. Since this term is much smaller than the nonlinear electric dipole polarization of a dipolar layer [27], it is possible to make thin enough liquid-crystal films for which the quadrupolar contribution to the second-harmonic signal can be neglected (see Sec. II B). The second-harmonic signal generated by mica [28] arises from the surface non-

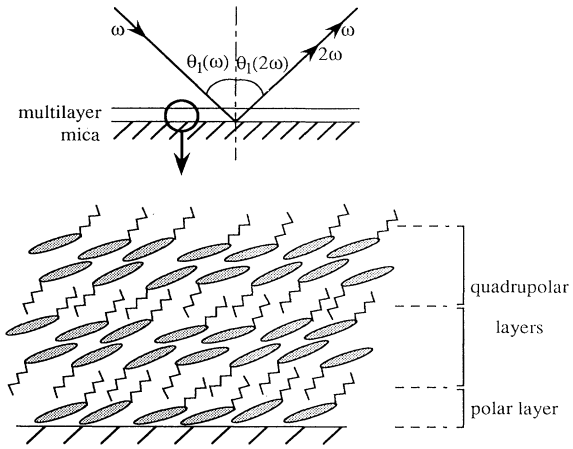


FIG. 1. Second-harmonic generation by a film of liquid-crystal molecules spread onto a mica surface together with the molecular structure of this film.

linearity induced by the structural asymmetry and field discontinuity existing at the mica surface [29]. This signal is, however, negligible compared to the signal generated by a liquid-crystal monolayer deposited onto the mica surface. Finally, the nonlinear susceptibility of volatile molecules such as the ethylene glycol molecules is too weak to yield a detectable second-harmonic signal.

In summary, the second-harmonic signal generated by a multilayer of cyanobiphenyl molecules deposited on mica corresponds essentially to the signal generated by the liquid-crystal monolayer adsorbed at the mica surface, which exhibits a certain degree of polar ordering [27]. The measurement of this signal can thus be used to probe specifically the behavior of this molecular monolayer.

The second-harmonic signal generated by a monolayer of liquid-crystal molecules [2] is proportional to $|\bar{\chi}^{(2)}_{\rm eff}|^2$, where $\bar{\chi}^{(2)}_{\rm eff}$ is the effective surface nonlinear susceptibility. This susceptibility is defined by

$$\bar{\chi}^{(2)}_{\rm eff}=[\hat{\mathbf{e}}(2\omega)\cdot\bar{\mathbf{L}}(2\omega)]\bar{\chi}^{D}:[\bar{\mathbf{L}}(\omega)\cdot\hat{\mathbf{e}}(\omega)][\bar{\mathbf{L}}(\omega)\cdot\hat{\mathbf{e}}(\omega)]\ , \tag{1}$$

where $\hat{\mathbf{e}}(\Omega)$ is the unit polarization vector for the incident beam ($\Omega=\omega$) or the second-harmonic beam ($\Omega=2\omega$), and $\bar{\mathbf{L}}(\Omega)$ are local-field tensors arising from the dielectric discontinuity at the surface [5].

The nonlinear dipolar susceptibility $\bar{\chi}^{D}$ of a monolayer of liquid-crystal molecules can be calculated from the second-order polarizability $\bar{\alpha}^{D}$ of one molecule [5]. For liquid-crystal molecules such as cyanobiphenyls, $\bar{\alpha}^{D}$ has one dominant element $\alpha^{D}_{\xi\xi\xi}$ along the long molecular axis $\hat{\xi}$ [30]. In this case, $\bar{\chi}^{D}$ takes the form

$$\chi^{D}_{ijk}=N_s\langle\alpha^{D}_{ijk}\rangle=N_s\langle(\hat{\mathbf{i}}\cdot\hat{\xi})(\hat{\mathbf{j}}\cdot\hat{\xi})(\hat{\mathbf{k}}\cdot\hat{\xi})\rangle\alpha^{D}_{\xi\xi\xi}\ , \tag{2}$$

where $N_s$ is the surface density of liquid-crystal molecules; $\hat{\mathbf{i}}$, $\hat{\mathbf{j}}$, and $\hat{\mathbf{k}}$ are unit vectors of the reference frame $(\hat{\mathbf{x}},\hat{\mathbf{y}},\hat{\mathbf{z}})$ of the substrate surface (Fig. 2), and $\langle\ \rangle$ denotes the average on all the surface molecules. Since the mica surface with which the liquid-crystal molecules interact has a $C_s$ symmetry [31], $\bar{\chi}^{D}$ has only six independent nonvanishing components [32]. In the reference frame of the substrate surface chosen such that the $x$ axis is parallel to the surface mirror plane, these components take the following form [4,5]:

$$\begin{aligned}
&\chi^{D}_{zzz}=N_s\langle\cos^3\theta\rangle\alpha^{D}_{\xi\xi\xi}\ ,\\
&\chi^{D}_{xxx}=-\tfrac{1}{4}N_s\langle\sin^3\theta(\cos3\phi+3\cos\phi)\rangle\alpha^{D}_{\xi\xi\xi}\ ,\\
&\chi^{D}_{zyy}=\chi^{D}_{yzy}=\chi^{D}_{yyz}\\
&\qquad=\tfrac{1}{2}N_s\langle(\cos\theta-\cos^3\theta)(1-\cos2\phi)\rangle\alpha^{D}_{\xi\xi\xi}\ ,\\
&\chi^{D}_{zxx}=\chi^{D}_{xzx}=\chi^{D}_{xxz}\\
&\qquad=\tfrac{1}{2}N_s\langle(\cos\theta-\cos^3\theta)(1+\cos2\phi)\rangle\alpha^{D}_{\xi\xi\xi}\ ,\\
&\chi^{D}_{zxz}=\chi^{D}_{zzx}=\chi^{D}_{xzz}=-N_s\langle(\sin\theta-\sin^3\theta)\cos\phi\rangle\alpha^{D}_{\xi\xi\xi}\ ,\\
&\chi^{D}_{xyy}=\chi^{D}_{yxy}=\chi^{D}_{yyx}=\tfrac{1}{4}N_s\langle\sin^3\theta(\cos3\phi-\cos\phi)\rangle\alpha^{D}_{\xi\xi\xi}\ ,
\end{aligned} \tag{3}$$

where $(\theta,\phi)$ are the spherical coordinates defining the molecular axis $\hat{\xi}$ (Fig. 2).

The full expression of $\bar{\chi}^{(2)}_{\rm eff}$ corresponding to a nonlinear susceptibility $\bar{\chi}^{D}$ of this form have been published elsewhere [5]. $\bar{\chi}^{(2)}_{\rm eff}$ depends on the angle $\Phi$ between the incident plane $(X,Z)$ of the laser beam and the mirror plane $(x,z)$ of the substrate surface (Fig. 2) via the local-field factors $\hat{\mathbf{e}}(2\omega)\cdot\bar{\mathbf{L}}(2\omega)$ and $\bar{\mathbf{L}}(\omega)\cdot\hat{\mathbf{e}}(\omega)$. Measuring the second-harmonic signal generated by a liquid-crystal monolayer as a function of $\Phi$ for four different combinations of input and output polarizations ($s$-in–$s$-out, $p$-in–$s$-out, $s$-in–$p$-out, $p$-in–$p$-out) and then fitting the obtained data with the corresponding expressions of $\bar{\chi}^{(2)}_{\rm eff}$ allows one to calculate the nonzero coefficients of $\bar{\chi}^{D}$. This gives the average values of different functions of cosines and sines of $\theta$ and $\phi$ [Eq. (3)], which yields information about the orientational distribution of the molecules in the monolayer.

In order to perform the second-harmonic generation measurements, we have used the usual setup [2] with a frequency-doubled ($\lambda=532$ nm) $Q$-switched, mode-locked, neodymium-doped yttrium aluminum garnet (Nd:YAG) laser (Quantronix 416) as the light source. Each $Q$-switch pulse consisted of around twenty 100-ps-long mode-locked pulses with a 14-ns separation between them. The repetition rate of the $Q$-switched pulses was 500 Hz and the energy per $Q$-switched pulse 0.6 mJ. The sample was mounted on a rotational stage in order to perform the second-harmonic-generation measurements as a function of $\Phi$.

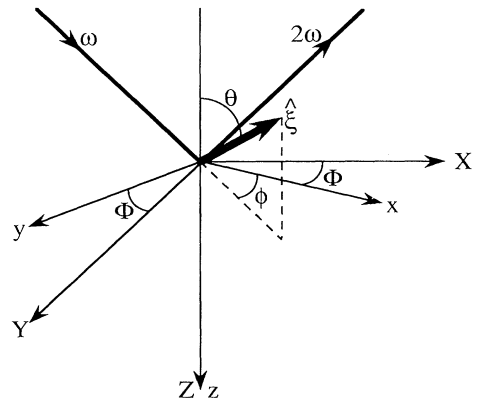


FIG. 2. Reference frames $(\hat{\mathbf{x}},\hat{\mathbf{y}},\hat{\mathbf{z}})$ of the substrate surface and $(\hat{\mathbf{X}},\hat{\mathbf{Y}},\hat{\mathbf{Z}})$ of the laboratory. $(X,Z)$ is the incident plane of the laser beam and $(x,z)$ the mirror plane of the substrate surface. The molecular axis $\hat{\xi}$ is defined with respect to the substrate axes by the spherical coordinates $(\theta,\phi)$.

### B. Samples

In order to study the effect of ethylene glycol on the anchoring of cyanobiphenyls on mica, we have observed the behavior of samples placed in a chamber with a controlled atmosphere. The composition of this atmosphere was determined by that of a slow lamellar flow of a mixture of dry nitrogen and nitrogen saturated in ethylene glycol [12]. The composition of the atmosphere in the

chamber can be characterized by the reduced partial pressure $\tilde{p}=p/p_s$, which is the ratio of the partial pressure $p$ over the saturation vapor pressure $p_s$ of ethylene glycol. Fixing $\tilde{p}$ corresponds to fixing the chemical potential of ethylene glycol in the system.

As substrates we have used 2- to 3-mm-thick cleaved muscovite mica plates which were kindly provided to us by D. Snowden-Ift (Department of Physics, University of California, Berkeley). The structure of muscovite mica has been extensively described elsewhere [21,24]. Muscovite mica is made of a stack of sheets, each of them having a mirror plane $\sigma$. The stack alternates sheets with two different mirror planes $\sigma_1$ and $\sigma_2$ separated by an angle of 120°. The resulting structure has a $C_{2h}^6$ symmetry with a glide plane $\Sigma$, which is the bisector of the two planes $\sigma_1$ and $\sigma_2$ (Fig. 3). The direction of $\Sigma$ in a given sample is easily found by means of a polarizing microscope, since it is perpendicular to the axis $\hat{\mathbf{b}}$ of the highest refractive index. The axis $\hat{\mathbf{c}}$ of the smallest refractive index makes an angle $\beta=5°$ with the sheets normal (Fig. 3). Mica cleaves easily and perfectly between two sheets creating two surfaces which are atomically smooth. One can make surfaces extending over 1 $cm^2$ without steps between different sheets.

As liquid crystals, we have used two different compounds, 5CB ($NC\Phi\Phi C_5H_{11}$) and 5OCB ($NC\Phi\Phi OC_5H_{11}$). The first one exhibits a nematic phase between 24 °C and 35 °C and the second one between 48 °C and 68 °C, with the possibility of supercooling the nematic phase of the latter down to 25 °C [33]. The macroscopic behavior of these two compounds is different when they are deposited on a freshly cleaved muscovite mica surface.

In an atmosphere of dry nitrogen, 5OCB orients perpendicular to the mirror plane $\sigma$ of the surface mica sheet. When ethylene glycol vapor is added, the system exhibits a first-order anchoring transition at a given reduced partial pressure $\tilde{p}_1$ of ethylene glycol. At this transition, the orientation of the nematic phase jumps abruptly to a direction parallel to $\sigma$. At a reduced pressure $\tilde{p}_2$ higher than $\tilde{p}_1$, the reverse transition is observed with the orientation of the nematic phase becoming again perpendicular to $\sigma$ [21]. With the mica used for the present study, we have also observed the same pair of transitions once or twice more when $\tilde{p}$ was further increased. The number of transitions observed depended on the time spent by the sample in the presence of ethylene glycol, probably because of contamination problems. The last transitions could only be observed if the sample was exposed to ethylene glycol for less than 30 min; the first one could be observed for 1 day. These transitions exhibit some hysteresis and the partial pressure of ethylene glycol at which they occur depends on the history of the sample. In particular, it is possible to keep the sample in a given state in the presence of ethylene glycol at a pressure $\tilde{p}$ and then induce the transition to the other state by perturbing for a short time the flow in the chamber (for instance, by a short interruption) while $\tilde{p}$ remains constant.

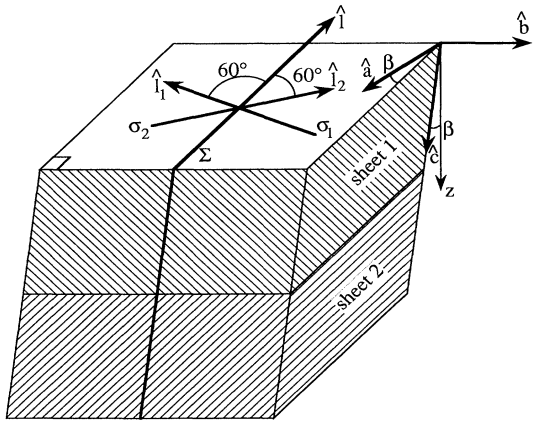


FIG. 3. Monoclinic elementary cell of muscovite mica. $\Sigma$, glide plane of the crystal; $\sigma_1$ and $\sigma_2$, mirror planes of the sheets forming the crystal; $\hat{\mathbf{a}}$, $\hat{\mathbf{b}}$, and $\hat{\mathbf{c}}$, optical axes of the crystal.

On the contrary, 5CB orients parallel to $\sigma$ in a dry atmosphere. When ethylene glycol vapor is added, the system exhibits a first-order anchoring transition at a given reduced pressure $\tilde{p}_0$, during which the orientation of the nematic phase jumps to a direction perpendicular to the mirror plane $\sigma$. A further increase of $\tilde{p}$ does not modify the anchoring conditions. This anchoring transition has a lifetime of 1 day.

For both 5OCB and 5CB, the nematic phase always remains oriented parallel to the mica surface. Moreover, the anchoring transitions are reversible and reproducible within the limit of their lifetimes.

In order to study the behavior at the anchoring transition of the liquid-crystal molecules in contact with the substrate surface by second-harmonic-generation measurements, films of liquid-crystal molecules are first deposited onto mica plates, in the presence of a dry atmosphere, by evaporating the liquid crystal from a hot source and letting it condense onto the plates. The deposition is monitored by measuring the second-harmonic signal generated by the film [34]. The signal first increases quadratically with time and then abruptly saturates indicating that a full monolayer has been formed onto the surface (Fig. 4).

If the evaporation goes on, two cases can occur. In 5OCB, the adsorption continues leading to the formation of a liquid-crystalline film with quadrupolar molecular ordering (Fig. 1) on top of the first polar monolayer. The additional layers add a contribution to the second-harmonic signal arising from the induced electric quadrupole polarization: $\mathbf{P}_Q^{(2)}(2\omega)=\bar{\chi}^Q:\mathbf{E}(\omega)\nabla\mathbf{E}(\omega)$. Since the majority of the molecules in the first monolayer point their cyanogroup (—CN) towards the substrate surface [27] and the molecules in the quadrupolar film point with their heads toward each other, the nonlinear polarization of the polar monolayer $\mathbf{P}_D^{(2)}$ and that of the quadrupolar film $\mathbf{P}_Q^{(2)}$ have opposite signs. The adsorption of molecules on top of the first monolayer leads thus to a small decrease of the second-harmonic signal. The ratio of the signal at the moment when the deposition is stopped over the signal from the first monolayer gives an estimate of the thickness of the liquid-crystalline film. The signal

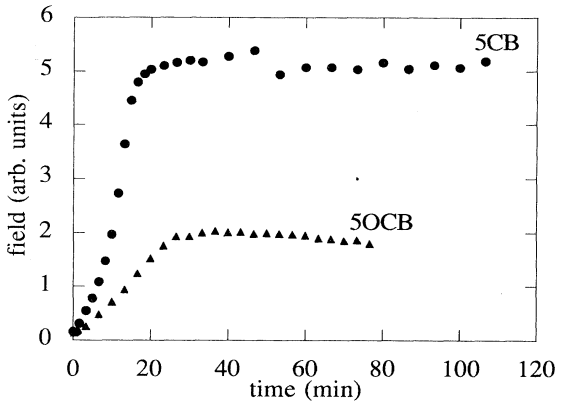


FIG. 4. Square root of the second-harmonic signal versus time during the deposition of 5OCB and 5CB molecules on mica.

$S(N)$ generated by a film made of one dipolar monolayer and $N$ quadrupolar bilayers [35,36] is roughly proportional to $|\chi^D+N\chi^Q k|^2E^2$, where $k$ is the wave number of the incident beam, $\chi^D$ and $\chi^Q \approx -\xi_0\chi^D$ are the effective susceptibility of a polar and a quadrupolar layer, respectively, and $\xi_0$ is the distance between two antiparallel molecules in the quadrupolar layers measured along their axis $\hat{\xi}$ [27]. For our experiments, we have made films such that $S(N)/S(0)\approx 0.8$. Since $\xi_0 \approx 15$ Å [27] and $k=2\pi/5320$ Å$^{-1}$, $N\approx(1/k\xi_0)[1-\sqrt{S(N)/S(0)}]\approx 6$, which corresponds to a thickness of approximately 160 Å. Neglecting the quadrupolar contribution to the second-harmonic signal in further analysis then leads to an error of approximately 10% on the determination of $\bar{\chi}^D$.

In the second case, observed with 5CB, the second-harmonic signal remains constant after saturation (Fig. 4). This means that no other layer adsorbs on top of the monolayer in contact with mica. Similar differences in adsorption behavior between $n$CB and $n$OCB compounds have already been observed [34].

The second-harmonic-generation measurements were performed at 28 °C for 5CB layers and 37 °C for 5OCB layers. In the latter case, the chosen temperature is lower than the melting temperature of the compound (but higher than the temperature down to which the nematic phase can be supercooled). We have checked that increasing the temperature above the melting temperature does not change the results of the measurements.

Each measurement was done in a sufficiently short time and the interval between two consecutive measurements was sufficiently long so that the laser beam would not locally heat the sample. Such a heating would induce the desorption of ethylene glycol molecules from the mica surface.

## III. RESULTS OF SECOND-HARMONIC-GENERATION MEASUREMENTS

### A. 5OCB

Figure 5 shows the square root of the second-harmonic signal (which is proportional to the absolute value of the effective susceptibility $\bar{\chi}^{(2)}_{\text{eff}}$ generated by a film of 5OCB on muscovite mica for different compositions of the atmosphere surrounding the system. In these plots $\Phi=0°$ refers to $\pm 60°$ (depending on the surface mica sheet) away from the crystallographic direction $\hat{l}$ of the muscovite mica defined in Fig. 3. This direction is determined from the anisotropy of the second-harmonic signal generated by the mica surface (see Fig. 16 and Appendix A). This means that the $\Phi=0°$ axis of the plots presented in Fig. 5 corresponds to either vector $\hat{l}_1$ or vector $\hat{l}_2$ belonging respectively to the mirror planes $\sigma_1$ and $\sigma_2$ of the mica sheets, depending on which kind of sheet is at the mica surface ($\sigma_1$ in the configuration shown in Fig. 3).

Figure 5(a) corresponds to the case of an atmosphere of dry $N_2$ obtained by having dry $N_2$ flowing directly into the chamber. Figure 5(b) corresponds to an atmosphere of dry $N_2$ with traces of ethylene glycol. It is obtained by sending into the chamber the mixture of a flow of dry $N_2$ and a flow of $N_2$ saturated in ethylene glycol, with the nominal composition 100%:0%. Due to an uncertainty of approximately 1% in the composition of the mixture, this is not equivalent to a pure flow of dry $N_2$. Adding traces of ethylene glycol in the atmosphere obviously does not introduce much change in the liquid-crystal monolayer. The main effect is a small decrease in the intensity of the second-harmonic signal. This decrease indicates that the number of liquid-crystal molecules constituting the polar monolayer in contact with the mica surface decreases when ethylene glycol molecules are added in the atmosphere.

When the reduced partial pressure of ethylene glycol is increased to approximately 10%, small changes in the shape of the second-harmonic signal are observed [Fig. 5(c)]. If the system is perturbed, while keeping the composition of the atmosphere constant, to induce a transition in the monolayer corresponding to the anchoring transition in the bulk (see Sec. II B), a significant change in the second-harmonic signal is observed [Fig. 5(d)]. First, the intensity of the signal decreases, indicating that a sudden decrease of the density of liquid-crystal molecules occurs. The $p$-out signals also exhibit a significant change in shape, which indicates a change in the orientational distribution of the liquid-crystal molecules. An orientational transition must have taken place in the monolayer.

When the partial pressure of ethylene glycol is further increased, the intensity of the second-harmonic signal slowly decreases until it becomes unmeasurable when $\tilde{p}$ reaches approximately 60%, while the shape of the signal does not significantly vary. All these changes are reversible provided the system has not been exposed to ethylene glycol too long (see Sec. II B).

If there is only one monolayer of 5OCB deposited into the mica surface, the second-harmonic signal is the same as that of a thicker film before the anchoring transition but totally disappears when the transition takes place, indicating that there are no more liquid-crystal molecules at the mica surface. This change is irreversible and going back to an atmosphere of pure $N_2$ does not restore the second-harmonic signal.

### B. 5CB

Figure 6 shows the square root of the second-harmonic signal generated by a monolayer of 5CB on muscovite mica surrounded by an atmosphere of dry nitrogen. Their angular dependence, in particular that of the *p*-out signals, differs significantly from those obtained for 5OCB monolayers in a dry atmosphere, indicating different orientational distributions of the molecules.

Adding ethylene glycol in the atmosphere with any concentration leads to the disappearance of the signal. Since it is not possible to make 5CB films more than one monolayer thick on muscovite mica (see Sec. II B) in order to have a reservoir of these molecules, it is not possible to follow the effect of volatile molecules on the surface monolayer of 5CB in contact with a muscovite mica.

## IV. DATA ANALYSIS: ORIENTATIONAL DISTRIBUTIONS IN LIQUID-CRYSTAL MONOLAYERS

In order to study quantitatively the behavior of liquid-crystal monolayers in contact with mica surfaces, we

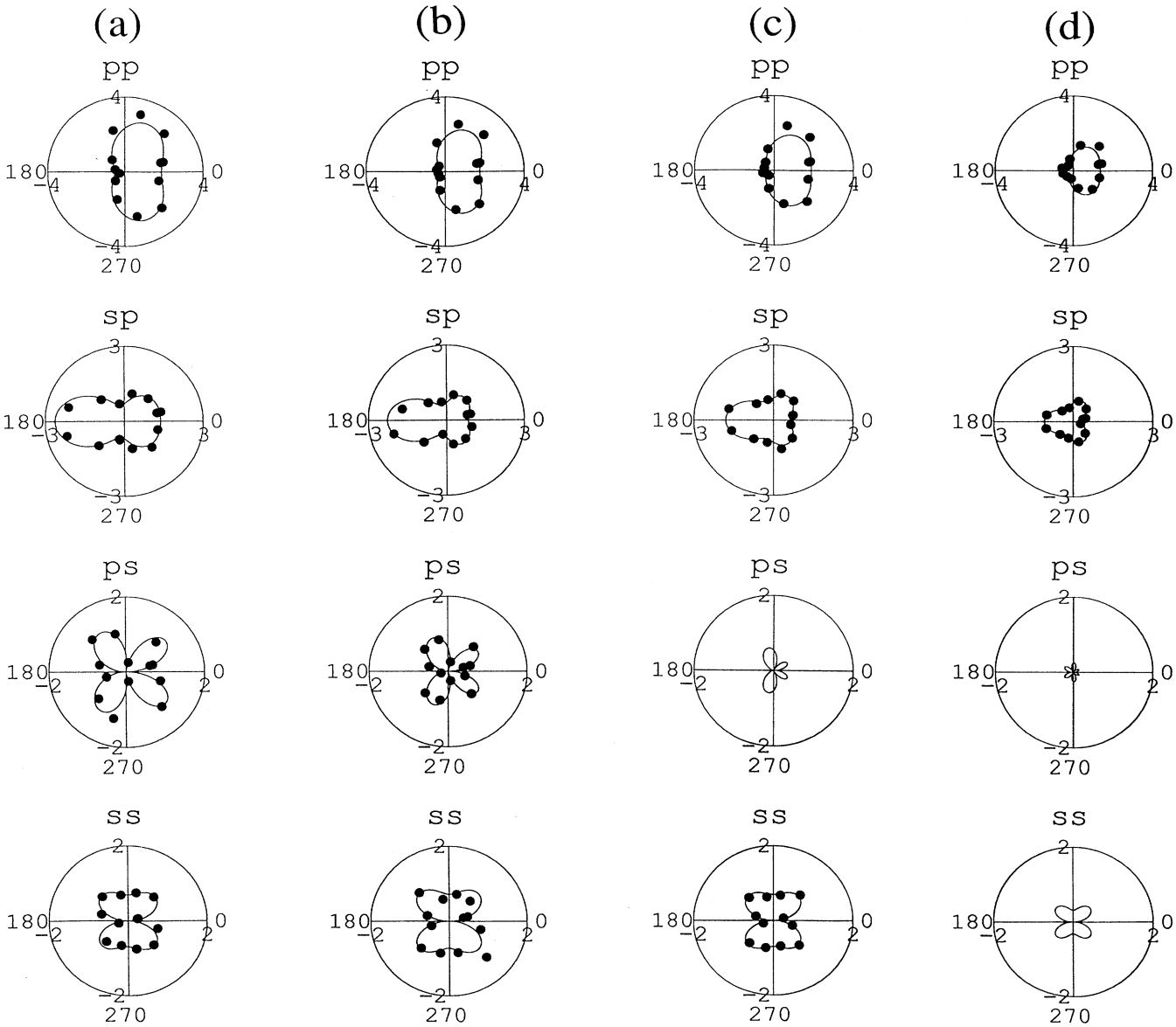


FIG. 5. Square root of second-harmonic signal (arbitrary units) versus angle $\Phi$ (defined in Fig. 2) from a 5OCB film deposited on muscovite mica (a) in dry $N_2$, (b) in $N_2$ with traces of ethylene glycol, (c) in $N_2$ with ethylene glycol at $\bar{p}=10\%$ before the anchoring transition, and (d) in $N_2$ with ethylene glycol at $\bar{p}=10\%$ after the anchoring transition. The markers correspond to the experimental data, the solid lines are the theoretical fits. The *p*-in–*s*-out signal in (c) and the *s*-out signals in (d) are too weak to be measured. $\Phi=0°$ in this figure corresponds to $\Phi=\pm 60°$ in Fig. 16 of Appendix A; the incidence plane is then parallel to the surface mirror plane.

have fitted the experimental second-harmonic generation data for different polarization combinations to calculate the various non-vanishing components of the nonlinear dielectric susceptibility $\bar{\chi}^D$ of the monolayer. For monolayers from which the second-harmonic signal was measurable only with two or three polarization configurations [Figs. 5(c) and 5(d)] instead of the complete set of four, $\bar{\chi}^D$ could still be calculated from the fit of two or three data sets. In the other cases, we could check that the results of the fit does not significantly depend on whether the data sets corresponding to an $s$-output polarization were used or not, as expected from the fact that $\bar{\chi}^D$ is highly overdetermined.

Once $\bar{\chi}^D$ is known for a given monolayer, one possesses via Eq. (3) some information about the orientational distribution of the molecules in the monolayer. In previous work using the same technique [4,5], it was assumed that this distribution took the following form:

$$f(\theta,\phi)=C\left[\exp\left[-\frac{(\theta-\theta_0)^2}{2\sigma^2}\right]\right]\times[1+d_1\cos\phi+d_2\cos2\phi+d_3\cos3\phi]\ , \tag{4}$$

where $C$ is a normalization constant and $\theta_0$, $\sigma$, and $d_i$ $(i=1,3)$ are parameters to be calculated. This form of $f(\theta,\phi)$ is not valid for the monolayers deposited on mica which we have studied. This can be seen by calculating the ratio

$$\frac{\langle\cos^3\theta\rangle}{\langle\cos\theta\rangle}=\frac{\chi^D_{zzz}}{\chi^D_{zzz}+\chi^D_{zxx}+\chi^D_{zyy}}\ . \tag{5}$$

This ratio is found to be negative for all the monolayers we have studied while it is always positive with the above distribution [Eq. (4)].

The main defect of the distribution given in Eq. (4) is that it implies that there are no liquid-crystal molecules oriented with their cyanogroup pointing away from the substrate surface ($90°\le\theta\le180°$). Indeed, since a majority of molecules are oriented with their cyanogroup towards the surface [27], $\theta_0$ is always found to belong to the interval $[0°,90°]$ and $f(\theta,\phi)$ is zero for $90°\le\theta\le180°$. This last condition implies that $\langle\cos\theta\rangle$ and $\langle\cos^3\theta\rangle$ are positive as well as $\langle\cos^3\theta\rangle/\langle\cos\theta\rangle$.

In order to get an "unbiased" estimate of the orientational distribution $f(\theta,\phi)$, i.e., one that does not rely on any *a priori* assumption, we have used the maximum-entropy method [38]. This method gives the widest distribution compatible with the available information on $f$. In our case, this information is the average values of the following functions [see Eq. (3)] obtained from the measurements of $\bar{\chi}^D$:

$$\begin{aligned}
&f_1(\theta,\phi)=\cos^3\theta\ ,\\
&f_2(\theta,\phi)=-\tfrac{1}{4}\sin^3\theta(\cos3\phi+3\cos\phi)\ ,\\
&f_3(\theta,\phi)=\tfrac{1}{2}(\cos\theta-\cos^3\theta)(1-\cos2\phi)\ ,\\
&f_4(\theta,\phi)=\tfrac{1}{2}(\cos\theta-\cos^3\theta)(1+\cos2\phi)\ ,\\
&f_5(\theta,\phi)=-(\sin\theta-\sin^3\theta)\cos\phi\ ,\\
&f_6(\theta,\phi)=\tfrac{1}{4}\sin^3\theta(\cos3\phi-\cos\phi)\ .
\end{aligned} \tag{6}$$

In order not to introduce any bias, we need to maximize the uncertainty on $f(\theta,\phi)$, defined by $H(f)=-\int_0^{\pi}\int_0^{2\pi}f(\theta,\phi)\ln[f(\theta,\phi)]\sin\theta\,d\theta\,d\phi$, with the known constraints on $\langle f_i(\theta,\phi)\rangle$ $(i=1,6)$. This is equivalent to maximizing the quantity $H-\sum_{i=1}^{6}\lambda_i f_i$, where $\lambda_i$ $(i=1,6)$ are Lagrangian multipliers. This maximization leads to

$$f(\theta,\phi)=\frac{\exp\left[\sum_{i=1}^{6}\lambda_i f_i(\theta,\phi)\right]}{\int_0^{\pi}\int_0^{2\pi}\exp\left[\sum_{i=1}^{6}\lambda_i f_i(\theta,\phi)\right]\sin\theta\,d\theta\,d\phi}\ , \tag{7}$$

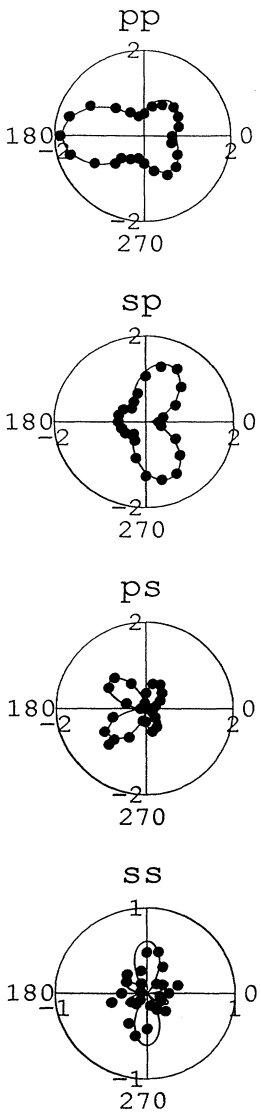


FIG. 6. Same as Fig. 5 for a 5CB layer on muscovite mica in dry $N_2$.

where $\lambda_i$ $(i=1,6)$ are to be calculated from the set of equations

$$\langle f_i(\theta,\phi)\rangle = \int_0^{\pi}\int_0^{2\pi} f_i(\theta,\phi) f(\theta,\phi)\sin\theta\, d\theta\, d\phi \qquad (i=1,6)\ . \quad (8)$$

For further discussion about the choice of orientational distribution see Appendix B.

In our case, the experimental measurements give the values of $\bar{\chi}_i^D = N_s\alpha_{\xi\xi\xi}^D\langle f_i(\theta,\phi)\rangle$ $(i=1,6)$. The product $N_s\alpha_{\xi\xi\xi}^D$ is not known since the second-harmonic signal is not measured in absolute units. We can calculate a minimum value for this product by considering the range of values each $\langle f_i(\theta,\phi)\rangle$ can have. For each value of $N_s\alpha_{\xi\xi\xi}^D$ above this minimum, we have determined the corresponding distribution $f(\theta,\phi)$. As $N_s\alpha_{\xi\xi\xi}^D$ increases, the height of the maxima of $f(\theta,\phi)$ is found to decrease while their positions remain approximately constant.

We will reproduce below the distributions calculated for the different monolayers we have studied with values of the product $N_s\alpha_{\xi\xi\xi}^D$ estimated as follows. Examination of the distributions calculated for the present study and the one calculated using the same method for formerly studied monolayers (see Appendix B) shows that the distribution in angle $\theta$ defined by $f_\theta(\theta)=\int_0^{2\pi} f(\theta,\phi)d\phi$ is approximately the same for all of them. Thus $\langle\cos^3\theta\rangle = \chi_1^D/N_s\alpha_{\xi\xi\xi}^D = \chi_{zzz}^D/N_s\alpha_{\xi\xi\xi}^D$ is essentially identical for all these distributions. The value of $\langle\cos^3\theta\rangle$ can be calculated from the case considered in Appendix B and the values of $N_s\alpha_{\xi\xi\xi}^D$ for each case then estimated.

### A. Results for 5OCB

Figure 7 gives the obtained orientational distributions $f(\theta,\phi)$ in 5OCB monolayers in the presence of atmospheres with increasing concentration of ethylene glycol; Fig. 8 summarizes the evolution of the peak positions in these distributions together with the proportion of molecules in each peak.

In all cases, the distribution exhibits a peak for orientations close to $\theta=180°$ for which the rigid core of the molecules is perpendicular to the surface with the cyano-group pointing away from it. The proportion of molecules in this peak ($\approx$24%) does not depend on the composition of the atmosphere. All the distributions also exhibit two other peaks symmetric with respect to $\phi=0°$ (only one appears in the plots). As the concentration of ethylene glycol in the atmosphere increases, the position of the latter peaks evolves, with their spherical coordinates $\theta$ and $\phi$ respectively increasing and decreasing (Fig. 8). The proportion of molecules in these peaks also decreases. Moreover a new peak at $\phi=180°$ and $\theta\approx 57°$

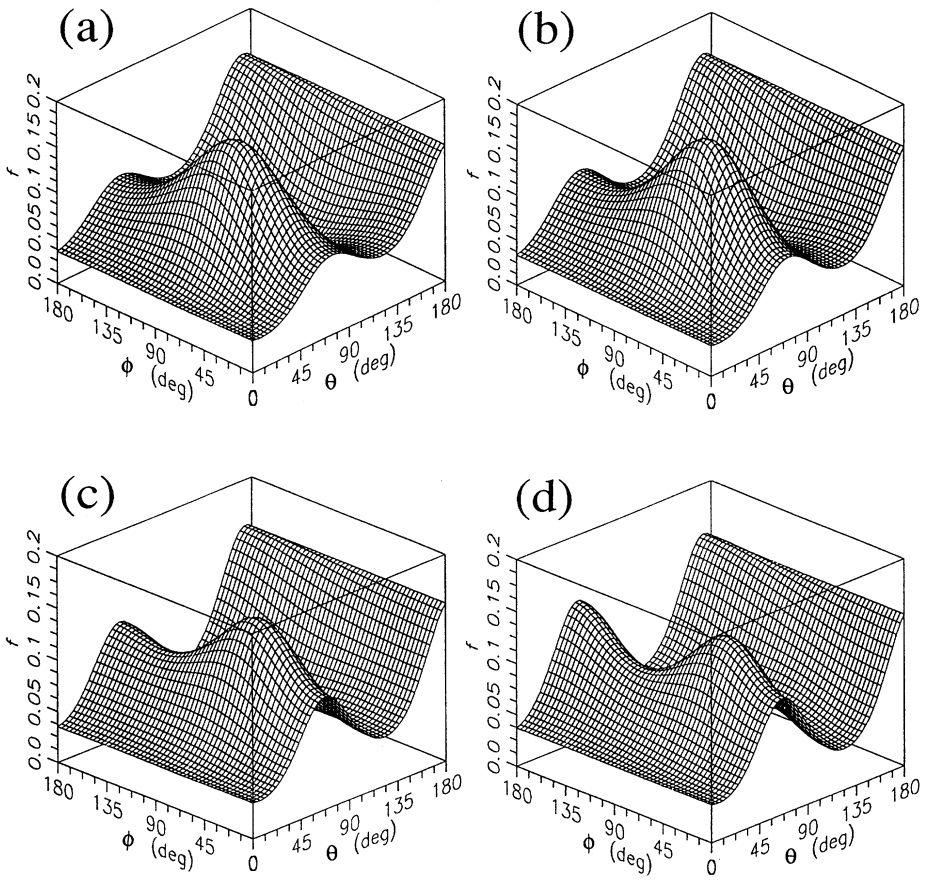


FIG. 7. Orientational distribution $f(\theta,\phi)$ of the molecules in 5OCB monolayers obtained from the data given in Fig. 5. For different samples, the position of the peaks are reproducible within $\pm 3°$ and the proportion of molecules in the peaks within $\pm 2\%$. The orientation of a molecule is given by a unit vector with spherical coordinates $(\theta,\phi)$ heading towards the aliphatic tail of the molecule. $\phi=0°$ corresponds to an orientation in the plane $\Phi=0°$ of Fig. 5. For clarity, $f(\theta,\phi)$ is plotted only for $0°\le\phi\le 180°$; the shape of $f(\theta,\phi)$ for $180°\le\phi\le 360°$ can be obtained by applying the mirror symmetry with respect to $\phi=180°$. Note that the lines $\theta=0°$ and $180°$ in the plots correspond in fact to one point in the space of orientations.

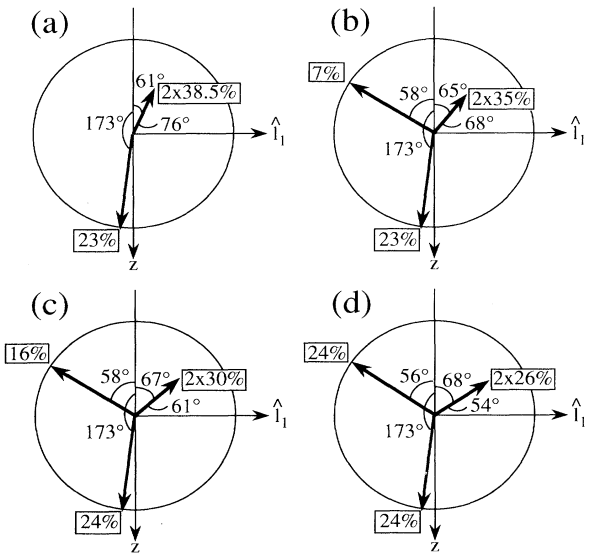


FIG. 8. Position of the different peaks and proportion of molecules in each peak for the distributions given in Fig. 7.

shows up [Figs. 8(b)–8(d)]. The proportion of molecules in this peak increases as the concentration of ethylene glycol increases.

The density of liquid-crystal molecules in the monolayer also varies when ethylene glycol is added in the atmosphere. From the estimated product $N_s\alpha^D_{\xi\xi\xi}$ for each monolayer (see above), one can calculate how the surface density $N_s$ of 5OCB in contact with the mica surface varies when the concentration of ethylene glycol increases. When ethylene glycol is first introduced, the surface density $N_s$ decreases by 20%. Upon increasing the concentration in ethylene glycol but keeping it below the value at which the anchoring transition occurs, $N_s$ decreases by a few percent. At the transition, the monolayer loses approximately 30% of the liquid-crystal molecules present before the transition.

### B. Results for 5CB

Figure 9 gives the orientational distribution $f(\theta,\phi)$ in a 5CB monolayer on muscovite mica in dry nitrogen. As expected from the shape of the second-harmonic signal, this distribution differs significantly from the distribution of a 5OCB monolayer in dry nitrogen [Fig. 7(a)].

## V. DISCUSSION: BEHAVIOR OF CYANOBIPHENYLS ON MUSCOVITE MICA

We now possess the following information concerning the behavior of cyanobiphenyl liquid crystals on muscovite mica in the presence of an atmosphere containing ethylene glycol vapor.

From a macroscopic point of view, a nematic film of 5OCB in the presence of a dry atmosphere orients along the mica surface and perpendicular to its mirror plane. When ethylene glycol is added with increasing concentration, a first-order anchoring transition takes place around a critical concentration, after which the planarly aligned nematic phase orients parallel to the surface mirror plane. When the concentration of ethylene glycol is further increased, a series of other transitions between anchoring directions perpendicular and parallel to the surface mirror plane can also be observed shortly after the system has been put in the presence of ethylene glycol. The nematic phase of 5CB exhibits only one anchoring transition with the orientation being parallel to the mirror plane before this transition and perpendicular to it after.

From a microscopic point of view, we know from second-harmonic-generation measurements the orientational distribution in the liquid-crystal monolayers in contact with the mica surface. In the case of 5OCB (Figs. 7 and 8), the monolayers were covered by a 160-Å-thick film of liquid crystal and surrounded by atmospheres with different compositions. In the case of 5CB (Fig. 9), the monolayer was not covered by other liquid-crystal molecules and could be studied only in a dry nitrogen atmosphere. For 5OCB, the presence of ethylene glycol molecules has a clear tendency to reorient the liquid-crystal molecules in the monolayer: it creates a peak in the orientational distribution for a molecular orientation in the mirror plane of the mica surface and it makes the peaks located outside this plane evolve towards this plane. Before the anchoring transition, the evolution of

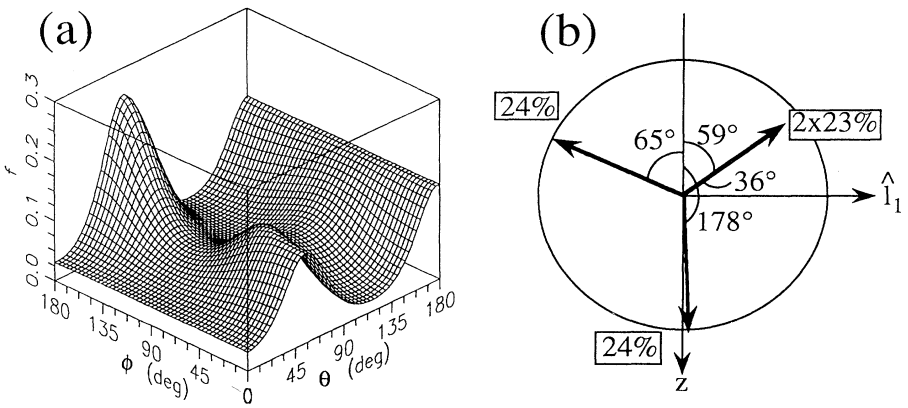


FIG. 9. (a) Orientational distribution $f(\theta,\phi)$ of the molecules in a 5CB monolayer obtained from the data given in Fig. 6. The conventions are the same as in Fig. 7. (b) Position of the different peaks and proportion of molecules in each peak for this distribution.

the orientational distribution is continuous, while at the transition, the distribution undergoes a discontinuous change. The density of liquid-crystal molecules in this monolayer also varies discontinuously at the transition.

In order to relate the microscopic behavior of surface monolayers to the macroscopic behavior of cyanobiphenyl liquid crystals on mica, we must assume that a monolayer of liquid crystal deposited on a substrate in the absence of bulk liquid crystal behaves the same way as a monolayer in the presence of bulk liquid crystal. Similar studies made on other substrates show that the presence of the bulk changes only slightly the orientational distribution of the molecules in the monolayer in contact with the substrate [4,5,27]. Moreover, for 5OCB in a dry atmosphere, the distributions we have found are the same whether the monolayer is covered with other liquid-crystal molecules or not. The above assumption is thus reasonable. As far as the adsorption of ethylene glycol is concerned, it can be argued that if the behavior of ethylene glycol at the mica–liquid-crystal interface is primarily determined by local interactions, this behavior should be essentially the same in the films we have studied and at the mica–bulk-liquid-crystal interface. In the present discussion, we will assume that this is indeed the case.

The first point of discussion concerns how the macroscopic anchoring direction imposed by the mica surface on the bulk liquid crystal is determined. It is indeed *a priori* surprising that the orientational distribution in the surface monolayer is found to exhibit so many peaks while the bulk liquid crystal takes one particular orientation. Such a well-defined bulk orientation occurs even when the surface monolayer is nearly isotropic [39]. In fact, in the case of a flat and smooth surface, the orientational distribution of the molecules in contact with the substrate plays the role of boundary condition for the field of molecular orientation in the bulk. The bulk has to remain uniaxial with a certain direction of orientation, which is determined by the adaptation of the liquid crystal to this boundary condition. One can consider that the bulk liquid crystal is epitaxially grown on top of the surface monolayer of liquid-crystal molecules [5,6]: the bulk liquid crystal chooses the orientation which minimizes its interaction with this monolayer.

In order to check quantitatively this idea, one can calculate the effective interaction potential of a bulk molecule with the surface monolayer in which the molecules exhibit one of the above calculated orientational distributions. We have taken a Maier-Saupe type [40] of interaction potential between two molecules whose orientations are represented by the unit vectors $\hat{\xi}$ and $\hat{\xi}'$, respectively: $v(\hat{\xi},\hat{\xi}')=-B(\hat{\xi}\cdot\hat{\xi}')^2$, where $B$ is a positive constant. Then the effective interaction potential of a molecule having an orientation $\hat{\xi}$ defined by the spherical coordinates $(\theta,\phi)$ with a monolayer of molecules having an orientational distribution $f(\theta_m,\phi_m)$ is

$$V_{\text{eff}}(\hat{\xi})=-B\int_0^{\pi}\int_0^{2\pi}[\sin\theta\sin\theta_m\cos(\phi-\phi_m)+\cos\theta\cos\theta_m]^2 f(\theta_m,\phi_m)\times\sin\theta_m\,d\theta_m\,d\phi_m\ . \quad (9)$$

We have plotted $-V_{\text{eff}}(\hat{\xi})/B$ as a function of $\theta$ and $\phi$ in Fig. 10 for 5OCB and Fig. 11(a) for 5CB. The maxima of these plots correspond to the most energetically favorable orientations for bulk molecules interacting with the considered monolayers; they are therefore the orientation chosen by the bulk liquid crystal, as predicted by this simple model [Figs. 12 and 11(b)].

In all cases, the predicted azimuthal orientation of the induced anchoring direction is in agreement with the experimental observations. In 5OCB, the anchoring direction is perpendicular to the surface mirror plane before the anchoring transition and parallel to it after; in 5CB, the anchoring direction is parallel to this plane in a dry atmosphere. As far as the tilt of the anchoring direction with respect to the surface is concerned, it is only correctly predicted for anchoring directions perpendicular to the mirror plane. In the other cases (5OCB after the transition and 5CB), the effective potentials have their minima for orientations tilted with respect to the substrate surface, which is in contradiction to the experimentally observed planar anchoring directions.

The causes of this discrepancy are certainly to be found in the defects of the model. First, this model takes into account only the rigid core of the molecules, i.e., the cyanobiphenyl group. A more realistic model should consider that the long axis of these molecules does not coincide with the long axis of their rigid core and that the aliphatic chains also play a role in the intermolecular interactions. Unfortunately we do not have any information about the configuration of the aliphatic chains in our system. A second defect of the above model is that it does not take into account the presence of the transition region between the nematic bulk and the surface layer. The bulk structure is assumed to extend up to this layer; this is a kind of Fowler approximation, where the substrate surface is replaced by the surface liquid-crystal monolayer. Such an approximation implies an unrealistic discontinuity between this layer and the rest of the liquid-crystalline phase. Finally the intermolecular potential between the bulk liquid-crystal molecules has been neglected.

Another point to discuss is the different behavior of 5OCB and 5CB molecules. These molecules differ only by the presence in the former of an oxygen atom located between the rigid cyanobiphenyl core and the aliphatic chain. Obviously, this particular atom plays an important role in the interaction between 5OCB molecules and mica. In the absence of other molecules at the interface, it seems to prevent the 5OCB molecules from aligning parallel to the surface mirror plane (compare Figs. 7(a) and 8(a), on the one hand, and Fig. 9, on the other hand).

We now discuss the influence of ethylene glycol molecules on the orientation of 5OCB at the mica surface. The decrease of the density of liquid-crystal molecules in the polar surface layer, which occurs when ethylene glycol molecules are added to the atmosphere, means that some of the liquid-crystal molecules initially in contact with the mica surface are replaced by ethylene glycol molecules. The surface monolayer then is composed of a mixture of liquid-crystal and ethylene glycol molecules.

That ethylene glycol molecules replace liquid-crystal

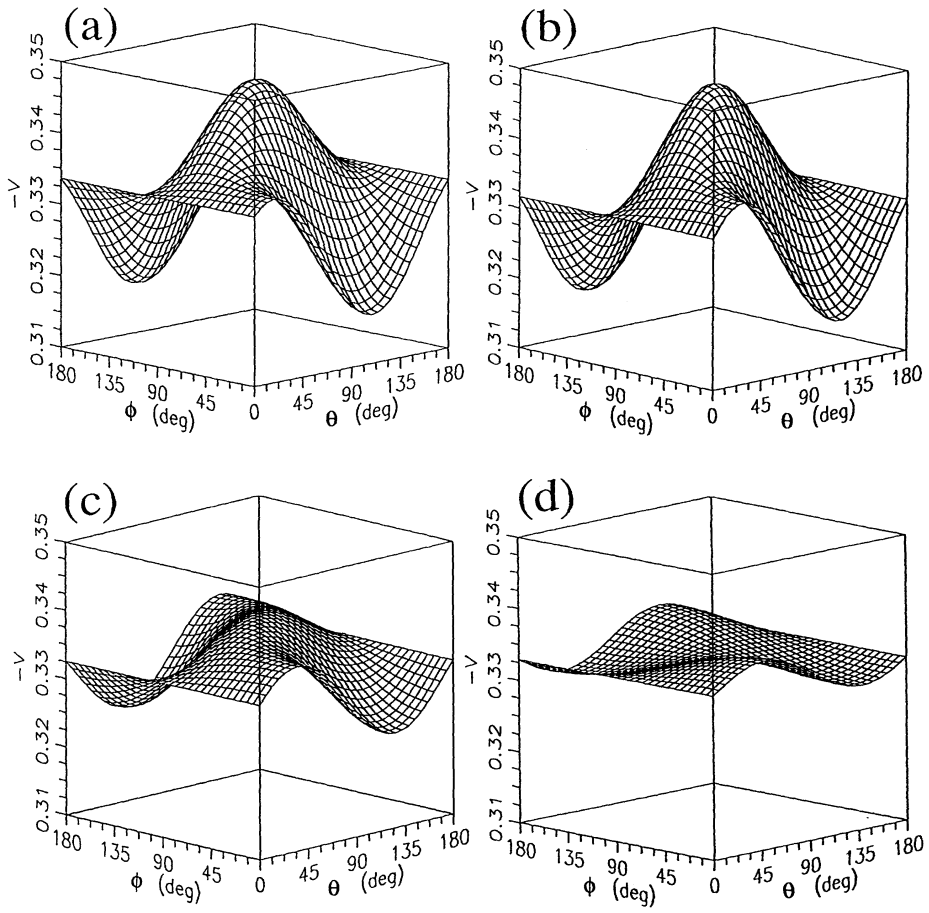


FIG. 10. Plot of the opposite of the effective interaction potentials $-V=-V_{\text{eff}}(\hat{\xi})/B$ between a molecule of orientation $\hat{\xi}(\theta,\phi)$ and the monolayers of 5OCB molecules whose orientational distributions are given in Fig. 7.

molecules at the mica surface can be understood if one considers the interactions between these molecules and mica. Cyanobiphenyl molecules interact with mica by van der Waals and dipole-ion interactions. Ethylene glycol molecules ($HOCH_2CH_2OH$) have the possibility of forming hydrogen bonds between the hydrogen atoms of their hydroxygroups (—OH) and the oxygen ions of the mica surface [21,24]. Since hydrogen bonds are stronger than van der Waals and dipole-ion interactions, the presence of ethylene-glycol molecules at the mica surface is favored with respect to that of liquid-crystal molecules [33]. Sum-frequency-generation measurements made on ethylene glycol molecules adsorbed on fused quarts [41] yield spectra with a peak corresponding to the $CH_2$ symmetric stretch mode. Since quartz and mica surfaces are chemically similar, ethylene glycol molecules should take the same configuration on both surfaces. The presence of this peak shows that the two $CH_2$ groups of the mole-

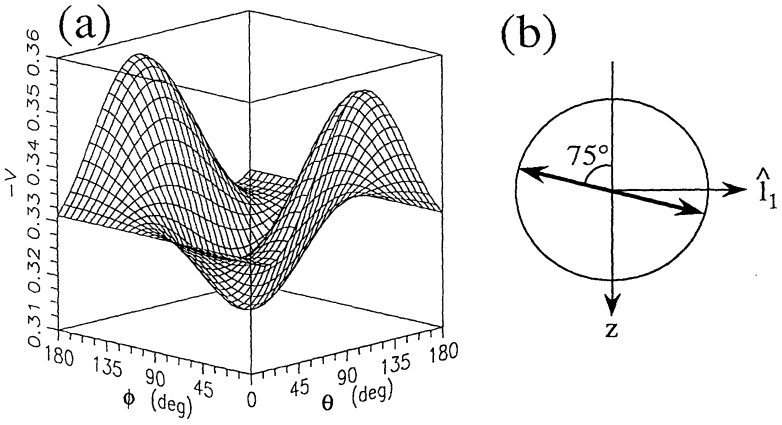


FIG. 11. Same as Figs. 10 and 12 for the monolayer of 5CB molecules whose orientational distribution is given in Fig. 9.

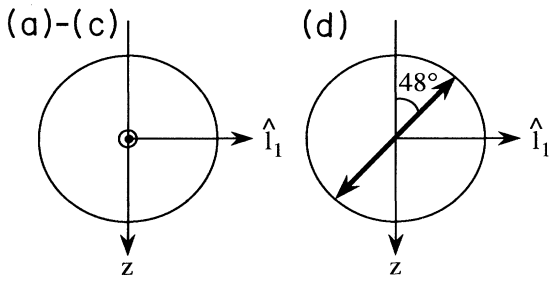


FIG. 12. Bulk orientation taken by 5OCB when its surface monolayer has one of the orientational distributions given in Fig. 7, as deduced from the interaction potential of a bulk molecule with the surface monolayer.

cules are oriented approximately in the same direction (otherwise the signals emitted by the two groups would have opposite phases and would cancel each other). This means that the two hydroxygroups both point towards the surface and form hydrogen bonds with oxygen atoms of the substrate surface; the $CH_2$ groups then point away from the substrate, making the surface nonpolar. Wherever ethylene glycol molecules are adsorbed on mica, the surface liquid-crystal monolayer loses the polar ordering it has when it is in direct contact with mica and no longer contributes to the second-harmonic generation.

Adsorbed ethylene glycol molecules act essentially on the azimuthal orientation of the surface liquid-crystal molecules, orienting them in three azimuthal directions $\phi = 180°$ and $\pm 60°$ (measured with respect to the surface mirror plane). Ethylene glycol has little effect on the tilt of the liquid-crystal molecules. In particular they do not affect the proportion of molecules oriented perpendicular to the surface. This is an indication that the replacement of surface liquid-crystal molecules by ethylene glycol molecules is independent of the tilt of the former.

Having the surface liquid-crystal molecules oriented along three directions making angles of 120° with each other is very unfavorable for the system: the interaction energies between the molecules in the monolayer and between these molecules and the bulk molecules are high. It is then more favorable for the system to switch to a state in which the two symmetric peaks make an angle with the mirror plane smaller than 60° [Fig. 7(d)]. At a critical ethylene glycol concentration, this induces a discontinuous change of the orientational distribution of the molecules in the first monolayer and hence a first-order anchoring transition during which the orientation of the bulk liquid crystal rotates by 90°. This discontinuous change in the induced anchoring direction must be associated with a discontinuous variation of the density of ethylene glycol adsorbed at the interface since these two variables are coupled (see Sec. I and [21]).

The above mechanism of anchoring transition accounts for a certain number of experimental observations concerning the transition of 5OCB from an orientation perpendicular to the surface mirror plane of mica to an orientation parallel to this plane when ethylene glycol is added. One can imagine that a similar mechanism (although working differently) could be responsible for the anchoring transition exhibited by 5CB under the same circumstances. Mechanisms of the same kind could surely account for the anchoring transitions observed when other volatile molecules are added, such as water and ethanol [33]. These molecules do not need to orient the surface liquid-crystal molecules in the same way as ethylene glycol molecules to induce the same changes in the anchoring direction, since a given anchoring direction can be the result of different orientational distributions of the molecules in contact with the substrate. As far as the successive anchoring transitions observed in 5OCB are concerned, they were not detected by second-harmonic-generation measurements, which might be because their lifetimes are too short with respect to the time needed to perform this type of measurements or because they occur when there are no more liquid-crystal molecules exhibiting a polar ordering to yield a second-harmonic signal.

In the following, we describe a possible microscopic mechanism leading to the reorientation of 5OCB molecules by ethylene glycol molecules along the azimuthal directions $\phi = 180°$ and $\pm 60°$ as considered above. This mechanism is based on the fact that the strongest interactions involved in our system are the hydrogen bonds linking the ethylene glycol molecules to the mica surface. These bonds should then determine the positions and orientations taken by the ethylene glycol molecules at the mica surface. Once these orientations are fixed, interactions between ethylene glycol and liquid-crystal molecules can lead to the reorientation of the liquid-crystal molecules. The orientations of the ethylene glycol molecules given here are deduced from qualitative considerations about the configuration of these molecules; they should be considered as possible orientations leading to the suited reorientations of the liquid-crystal molecules. The actual orientations of the ethylene glycol molecules might be determined from infrared or sum-frequency-generation spectroscopy or calculated by simulating the interactions of such molecules with mica.

The configuration taken by ethylene glycol molecules at the mica surface must be the one closest to the configuration of a free molecule while satisfying the condition that the two hydroxy groups point towards the surface (see above). In the configuration adopted by a free molecule, the O—H bonds are essentially parallel to the C—C bond [Fig. 13(a)]. The most favorable way of getting the O—H bonds directed towards the surface is to rotate them by $\pi$ around the C—O bonds. The O—H bonds then minimize their interactions with the other hydrogen and oxygen atoms of the molecule [Fig. 13(b)].

The hydrogen bonds linking an ethylene glycol molecule to mica should preferably be directed in the same direction as the O—H bonds of the ethylene glycol molecule and in the plane perpendicular to the plane containing the Si—O bonds in mica. Moreover, the hydrogen bonds must be around 2.8 Å long [42]. One can calculate the optimum location of oxygen ions with respect to an ethylene glycol molecule and then look for positions of this molecule with respect to the mica surface for which mica oxygen ions are approximately at these locations.

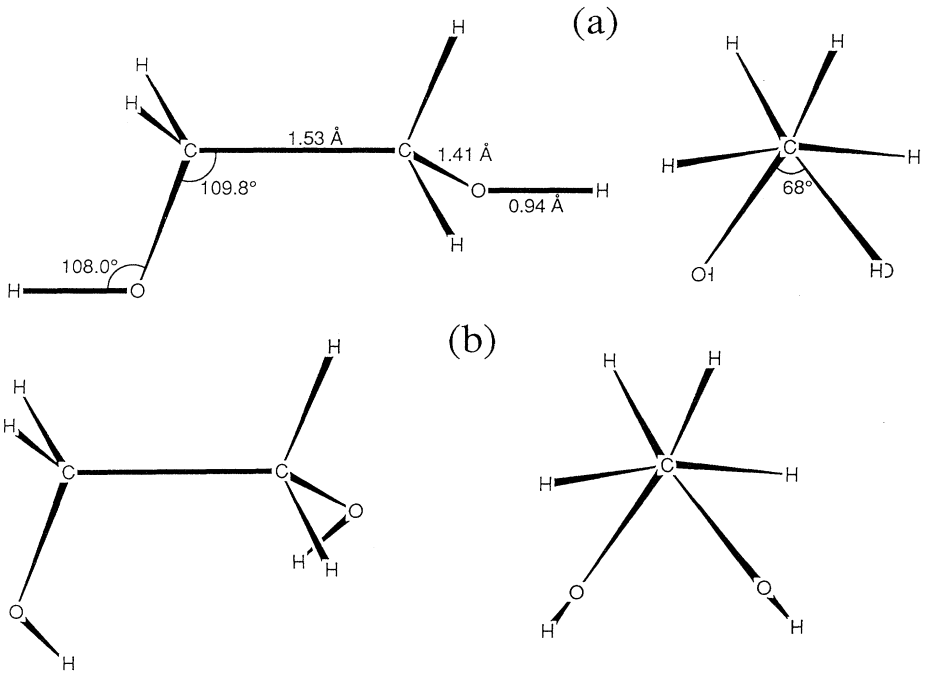


FIG. 13. Configuration of ethylene glycol molecules: (a) free molecule; (b) molecule at a mica surface derived from the former configuration by rotation of the O—H bonds by $\pi$ around the C—O bonds.

One such position is represented in Fig. 14(a); there are five equivalent ones found by rotating the molecule by $\pm 2\pi/3$ around the surface normal and/or taking the image of it in the plane containing the C—C bond. This position is not totally satisfactory since the hydrogen bonds are not in the right direction with respect to the Si—O bonds of mica and the oxygen atoms of the ethylene glycol molecule are close to oxygen ions of the mica surface. Considering that the oxygen-oxygen repulsion is stronger than the repulsion between other pairs of atoms and ions, the most probable position close to the former one is found by setting the oxygen atoms of the ethylene glycol molecule at equidistant positions from their two nearest mica oxygen ions [Fig. 14(b)]. There are in total six such positions corresponding to orientations in which the C—C bonds of the ethylene glycol molecules make an angle of $\pm 1°$, $\pm 59°$, or $\pm 61°$ with respect to the mirror plane of the mica surface.

Once the orientations taken by the ethylene glycol molecules on mica are known, one can consider how these molecules can affect the orientation of the liquid-crystal molecules at the mica surface. In bulk, the interactions between liquid-crystal and small solute molecules orient the solute molecules in a particular direction [43]. In general, the chosen orientation is found by projecting the solute molecule made of van der Waals spheres onto the plane perpendicular to the director for all possible orientations of the molecule and calculating for each orientation the circumference of the projected molecule. The chosen orientation is the one for which this circumference is the smallest [43]. For solute molecules which are slightly elongated, such as ethylene glycol molecules, this is a way of finding the "long" axis of the molecules which aligns parallel to the nematic director.

We can use a two-dimensional equivalent of this method to find the most favorable relative orientation of the ethylene glycol and liquid-crystal molecules at the mica surface. The shape of ethylene glycol molecules (made of van der Waals spheres) projected onto the mica surface (Fig. 15) is known from the configuration of these molecules at the mica surface described above [Fig. 13(b)]. This shape can be projected onto a line perpendic-

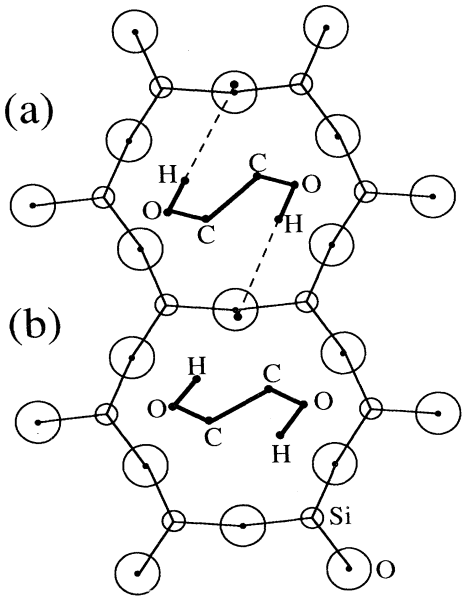


FIG. 14. Position of ethylene glycol molecules (projected on the surface plane) with respect to the mica surface: (a) determined from the most favorable location of mica oxygen ions with respect to an ethylene-glycol molecule for establishing hydrogen bonds; (b) alteration of the former position to minimize the repulsion between the mica oxygen ions and the oxygen atoms of the ethylene glycol molecule.

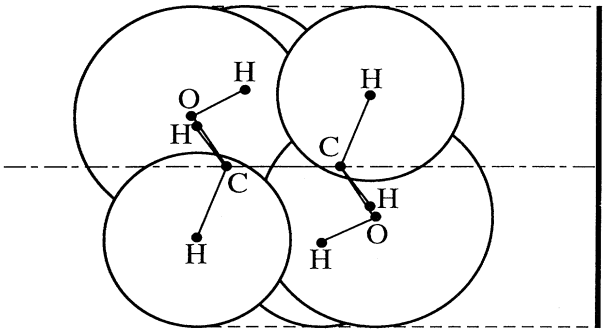


FIG. 15. Projection onto the mica surface of an ethylene glycol molecule made of van der Waals spheres having the configuration given in Fig. 13(b). The minimum width of the molecules corresponds to the molecular dimension perpendicular to the C—C bond.

ular to the axis of the liquid-crystal molecules with which the ethylene glycol molecule interacts. The direction of projection for which the width of the projected shape is minimum corresponds to the long axis of the ethylene glycol molecule. This axis is found to coincide with the C—C bond of the ethylene glycol molecule (Fig. 15). Ethylene glycol molecules having orientations equivalent to the one given in Fig. 14(b) thus tend to orient liquid-crystal molecules along the azimuthal directions $\phi = 180°$ and $\pm 60°$.

## VI. CONCLUSIONS

From the present study of the surface orientational distribution of liquid-crystal molecules on mica, we can draw several conclusions about surface behavior in liquid crystals.

The first ones concern anchoring. Our measurements show that while muscovite mica induces a unique anchoring direction in bulk cyanobiphenyl nematic liquid crystals, the liquid-crystal monolayer in direct contact with this substrate exhibits an orientational distribution with several peaks. A monostable macroscopic anchoring, i.e., a unique anchoring direction for the bulk liquid crystal, can result from a multistable microscopic anchoring, i.e., several possible orientations for molecules in contact with the substrate surface. The chosen macroscopic orientation arises from the adaptation of the uniaxial bulk structure to the microscopic anchoring conditions at the surface. Our measurements also show that anchoring conditions can greatly depend on the detailed molecular structure of the liquid crystal. Small changes in this structure can lead to significant modifications of the surface orientational order and thus of the macroscopic anchoring conditions.

Another conclusion concerns the interactions at surfaces between liquid-crystal and small nonmesogenic molecules. Although the latter exhibit no long-range orientational order, they become oriented when dissolved in bulk liquid crystals [43]. Our observations demonstrate that this orientation process can be reversed at surfaces, the small molecules affecting the orientational order of the liquid-crystal molecules. This can happen when the former interact more strongly with the substrate than the latter.

The other conclusions concern more specifically the adsorption-induced anchoring transitions observed on mica when volatile molecules are added in the atmosphere surrounding the system. Our observations justify *a posteriori* the name given to these transitions since the volatile molecules (ethylene glycol in our case) are indeed found to adsorb at the mica surface and to replace part of the liquid-crystal molecules initially in direct contact with mica. The presence of these small molecules induces a first-order transition in the surface monolayer characterized by a discontinuous change of the orientational order of the liquid-crystal molecules in this monolayer. This surface transition drives the reorientation of the bulk liquid crystal characterizing the previously observed anchoring transition. Another feature of the surface transition is that it is coupled to a discontinuous adsorption of volatile molecules, as predicted by thermodynamic considerations.

## ACKNOWLEDGMENTS

This work was supported by National Science Foundation (DMR-9025106). The mica plates were kindly provided to us by D. Snowden-Ifft (Department of Physics, University of California at Berkeley). B.J. acknowledges support from the Centre National de la Recherche Scientifique (France) and the Stichting voor Fundamenteel Onderzoek der Materie, which is financially supported by the Nederlandse Organisatie voor Wetenschappelijk Onderzoek (The Netherlands). B.J. is also grateful to J. Commandeur for helping with molecular modeling and to A. Alavi, B. Mulder, T. J. Sluckin, and P. I. C. Teixeira for fruitful discussions.

## APPENDIX A: SECOND-HARMONIC GENERATION BY MICA SURFACES

The second-harmonic signal generated by the muscovite mica surface is detectable only with input and output *p*-polarized beams. Because of the weakness of this signal and the high sensitivity of surface second-harmonic generation to impurities adsorbed onto the surface, the dependence of the signal upon rotation of the sample about its normal is not reproducible. To eliminate the noise in this signal, we have performed four successive measurements, peeling off a few mica layers between each measurement. The average of these four signals gives the signal generated by the mica surface itself (Fig. 16). This signal exhibits a mirror symmetry with respect to the $\Phi = 0°$ axis since this axis corresponds to the glide plane $\Sigma$ of the mica crystal and is larger for $\Phi = 0°$ than for $\Phi = 180°$. This anisotropy allows one to determine the orientation of the axis $\hat{c}$ of the smallest refractive index in the glide plane $\Sigma$ (Fig. 3) and thus the orientation of the liquid-crystal molecules with respect to the mica axes. For this purpose we need to calculate the second-harmonic signal generated by the mica surface.

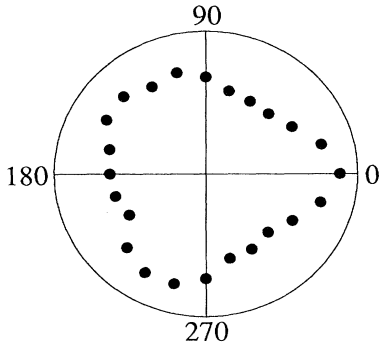


FIG. 16. Square root of the second-harmonic signal generated in the $p$-in–$p$-out polarization configuration by the muscovite mica surface. $\Phi=0$ corresponds to the glide plane $\Sigma$ of the mica crystal.

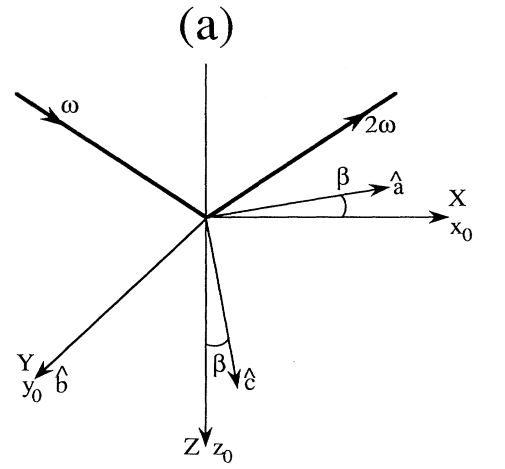


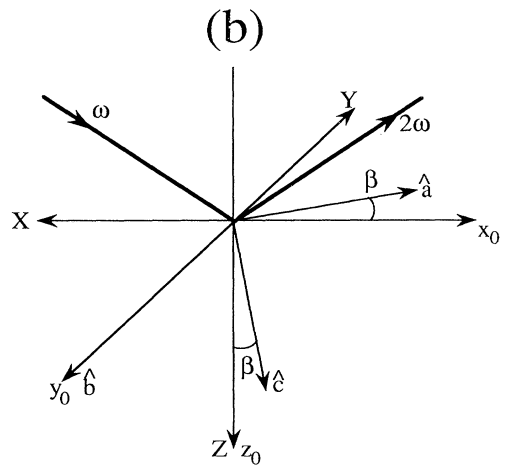


FIG. 17. Relative orientations of the beam reference frame $(\hat{\mathbf{X}},\hat{\mathbf{Y}},\hat{\mathbf{Z}})$, the surface reference frame $(\hat{\mathbf{x}}_0,\hat{\mathbf{y}}_0,\hat{\mathbf{z}}_0)$, and the optical axes $(\hat{\mathbf{a}},\hat{\mathbf{b}},\hat{\mathbf{c}})$ of the crystal for (a) $\Phi_0=\angle(\hat{\mathbf{x}}_0,\hat{\mathbf{X}})=0°$ and (b) $\Phi_0=180°$.

We have to calculate the second-harmonic signal generated by the surface of a centrosymmetric, anisotropic crystal in the following configuration. The axis $\hat{\mathbf{b}}$ of the largest refractive index $n_l$ of this crystal is parallel to the crystal surface $(x_0,y_0)$ with $\hat{\mathbf{b}}=\hat{\mathbf{y}}_0$ (Figs. 17 and 3). The axis $\hat{\mathbf{c}}$ of the smallest refractive index $n_s$ makes an angle $\beta$ with the surface normal $\hat{\mathbf{z}}_0$ and the third optical axis $\hat{\mathbf{a}}$ corresponding to the intermediate index $n_m$ makes the same angle with $\hat{\mathbf{x}}_0$. The incident plane of the fundamental beam is defined by the axes $\hat{\mathbf{X}}$ and $\hat{\mathbf{Z}}$ with $\hat{\mathbf{Z}}=\hat{\mathbf{z}}_0$. We shall consider only the configurations $\hat{\mathbf{X}}=\hat{\mathbf{x}}_0$ $(\Phi_0=0°)$ and $\hat{\mathbf{X}}=-\hat{\mathbf{x}}_0$ $(\Phi_0=180°)$ in which the incidence plane coincides with the glide plane $\Sigma=(\hat{\mathbf{a}},\hat{\mathbf{c}})$ of the crystal. Considering that in muscovite mica $n_l-n_m=6\times10^{-3}$ and $n_l-n_s=4\times10^{-2}$ [24], we assume for simplicity that $n_m=n_l=n_{ab}$ and write $n_s=n_c<n_{ab}$.

It has been shown that the second-harmonic signal generated by the surface layer of a centrosymmetric medium is the same as the signal generated by a sheet with an effective surface nonlinear susceptibility $\bar{\chi}^s$ related to the bulk nonlinear susceptibility of the medium [29]. We can therefore model the system by a polarizable sheet embedded in a dielectric medium with a dielectric tensor $\bar{\epsilon}^{(2)}$ located on top of a semi-infinite medium with the same dielectric tensor $\bar{\epsilon}^{(2)}$ (Fig. 18).

Moreover, when the incident fundamental beam is perpendicular to one of the optical axes of the medium, which is the case in the two configurations under consideration, the $p$ and $s$ components of the field are refracted independently. Therefore, the situation is essentially identical to the case of an isotropic medium except for the expression of $\bar{\epsilon}^{(2)}$ and we can follow the same procedure to calculate the second-harmonic signal generated by the surface as in the isotropic case [2,23].

Let $\mathbf{P}^s(X,Y)\delta(Z)=\mathbf{p}^s(X,Y)\delta(Z)\exp(ik_X X-i\omega_s t)$ be the polarization of the surface sheet. $\mathbf{P}^s$ is a nonlinear polarization at frequency $\omega_s=2\omega$ induced by a field at frequency $\omega$ incident from air (medium 1): $\mathbf{P}^s(2\omega)$

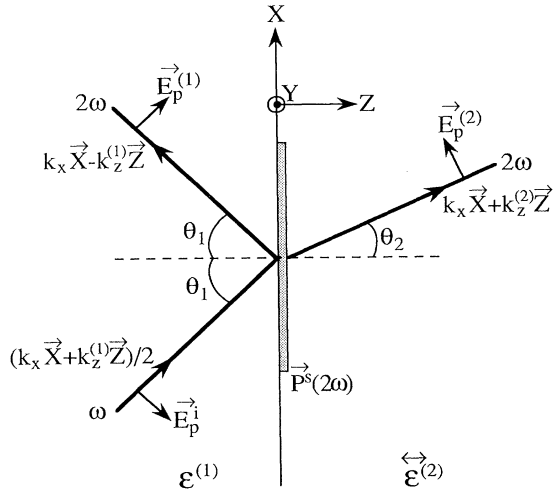


FIG. 18. Model system for calculating the second-harmonic signal generated by the surface of a medium with dielectric tensor $\bar{\epsilon}^{(2)}$. The other medium is isotropic and has a dielectric constant $\epsilon^{(1)}$.

$=\bar{\chi}^s:\mathbf{E}^s(\omega)\mathbf{E}^s(\omega)$, where $\bar{\chi}^s$ is the nonlinear susceptibility of the surface sheet and $\mathbf{E}^s$ is the fundamental field in this sheet. $\mathbf{E}^s$ is related to the incident field in air $\mathbf{E}^i$ by the Fresnel coefficients determining the refraction of a beam at the interface between the isotropic medium 1 and the anisotropic medium 2. In the case of a $p$-polarized incident beam $\mathbf{E}_p^i$, the refracted beam is also $p$ polarized and one writes

$$
\begin{aligned}
E_X^s &= 2E_p^i \cos\theta_1 \sin\theta_1 [-(n_{ab}^2 \sin^2\beta + n_c^2 \cos^2\beta)\cos\theta_2 + \eta(n_{ab}^2 - n_c^2)\cos\beta \sin\beta \sin\theta_2] \\
&\quad \times [(n_{ab}^2 \sin^2\beta + n_c^2 \cos^2\beta)\sin\theta_1 \cos\theta_2 + n_{ab}^2 n_c^2 \cos\theta_1 \sin\theta_2 - \eta(n_{ab}^2 - n_c^2)\cos\beta \sin\beta \sin\theta_1 \sin\theta_2]^{-1} , \\
E_Z^s &= 2E_p^i \cos\theta_1 \sin\theta_1 [(n_{ab}^2 \cos^2\beta + n_c^2 \sin^2\beta)\sin\theta_2 - \eta(n_{ab}^2 - n_c^2)\cos\beta \sin\beta \cos\theta_2] \\
&\quad \times [(n_{ab}^2 \sin^2\beta + n_c^2 \cos^2\beta)\sin\theta_1 \cos\theta_2 + n_{ab}^2 n_c^2 \cos\theta_1 \sin\theta_2 - \eta(n_{ab}^2 - n_c^2)\cos\beta \sin\beta \sin\theta_1 \sin\theta_2]^{-1} ,
\end{aligned}
\tag{A1}
$$

with $\eta=1$ for $\Phi_0=0°$ and $\eta=-1$ for $\Phi_0 180°$. All refractive indexes are at frequency $\omega$. The refraction angle $\theta_2$ is defined by the relation $n^{(2)}(\theta_2)\sin\theta_2=\sin\theta_1$ where the index $n^{(2)}(\theta_2)$ is the index in medium 2 for a $p$-polarized beam propagating in the plane of incidence making an angle $\theta_2$ with the $Z$ axis. $\theta_2$ is different for $\Phi_0=0°$ and 180°. For $n_{ab}=n_c$ and $\beta=0°$, Eq. (A1) reduces to the usual Fresnel factors for isotropic media [5].

Because the second-harmonic signal generated by the mica surface is detectable only for $p$-polarized input and output beams, the only non-negligible components of the surface nonlinear susceptibility $\bar{\chi}^s$ in the reference frame $(\hat{\mathbf{x}}_0,\hat{\mathbf{y}}_0,\hat{\mathbf{z}}_0)$ of the surface are $\chi^s_{z_0z_0z_0}, \chi^s_{z_0z_0x_0} = \chi^s_{z_0x_0z_0}, \chi^s_{z_0z_0y_0} = \chi^s_{z_0y_0z_0}$. Moreover the glide plane $\Sigma$ of the crystal corresponding to the plane $(x_0,z_0)$ is a mirror plane of the surface layer generating the second-harmonic signal, which imposes $\chi^s_{z_0z_0y_0} = \chi^s_{z_0y_0z_0} = 0$. For further simplification, we use the fact that the coupling between the field components parallel to the mica sheets and the polarization component perpendicular to them should be very weak, since these sheets are nearly independent of one another. Therefore $\chi^s_{z_0z_0x_0} = \chi^s_{z_0x_0z_0}$ is much smaller than $\chi^s_{z_0z_0z_0}$ and can be neglected. The nonlinear polarization of the surface sheet is thus parallel to the $z_0$ axis with $p^s_{z_0} = p^s_Z = \chi^s_{z_0z_0z_0}(E^s_{z_0})^2 = \chi^s_{z_0z_0z_0}(E^s_Z)^2$.

Once $\mathbf{P}^s$ is known, the field radiated by the polarization sheet in medium 1 can be calculated from the boundary conditions on the fields at the crystal-air interface. They are obtained from the following relations derived from integrations of the Maxwell equations over some volume $V$ enclosed in a surface $S$ or over a surface $S'$ specified by a contour $C$, all of them enclosing part of the interface:

$$
\begin{aligned}
&\oint_S \mathbf{B}\cdot d\mathbf{S} = 0 , \\
&\oint_C \mathbf{H}\cdot d\mathbf{l} = \frac{1}{c}\oint_{S'} \frac{\partial \mathbf{D}}{\partial t}\cdot d\mathbf{S}' , \\
&\oint_S \mathbf{D}\cdot d\mathbf{S} = 4\pi \int_V (-\nabla\cdot\mathbf{P}) dV , \\
&\oint_C \mathbf{E}\cdot d\mathbf{l} = -\frac{1}{c}\oint_{S'} \frac{\partial \mathbf{B}}{\partial t}\cdot d\mathbf{S}' .
\end{aligned}
\tag{A2}
$$

By adding to these relations the condition of continuity across the interface for $\mathbf{B}$, $E_X$, $E_Y$, and $D_Z$ ($\int_{0-}^{0+} F\,dZ = 0$ for a continuous component $F$), one obtains

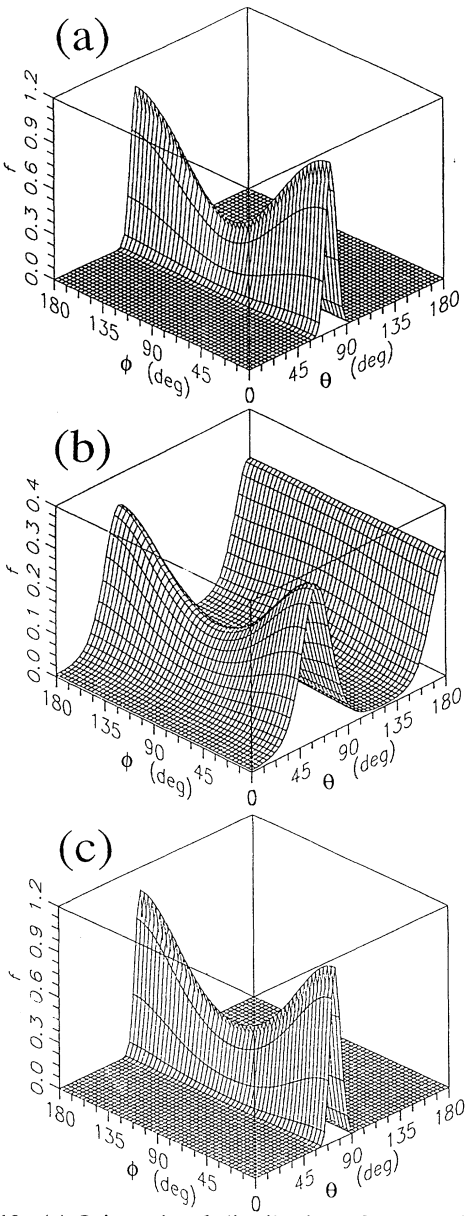


FIG. 19. (a) Orientational distribution of 8CB molecules on rubbed polyimide as calculated in [4,5]; (b) orientational distribution of the same system as calculated using the maximum-entropy method [Eq. (7)]; (c) the same as (b), but assuming $f(\theta,\phi)=0$ for $90° \le \theta \le 180°$. The reference frame is the same as in Figs. 7 and 9.

$$\Delta B_X=-4\pi i\frac{\omega_s}{c}P_Y^s+4\pi i\frac{\omega_s}{c}\frac{\epsilon_{YZ}^{(2)}(\omega_s)}{\epsilon_{ZZ}^{(2)}(\omega_s)}P_Z^s ,$$

$$\Delta B_Y=4\pi i\frac{\omega_s}{c}P_X^s-4\pi i\frac{\omega_s}{c}\frac{\epsilon_{XZ}^{(2)}(\omega_s)}{\epsilon_{ZZ}^{(2)}(\omega_s)}P_Z^s ,$$

$$\Delta B_Z=0 ,$$

$$\Delta E_X=-\frac{4\pi}{\epsilon_{ZZ}^{(2)}(\omega_s)}\frac{\partial P_Z^s}{\partial X} , \tag{A3}$$

$$\Delta E_Y=-\frac{4\pi}{\epsilon_{ZZ}^{(2)}(\omega_s)}\frac{\partial P_Z^s}{\partial Y} ,$$

$$\Delta D_Z=-4\pi\left[\frac{\partial P_X^s}{\partial X}+\frac{\partial P_Y^s}{\partial Y}\right] ,$$

where $\Delta F$ stands for $F(Z=0^+)-F(Z=0^-)$. Except for the second term in the expressions of $\Delta B_X$ and $\Delta B_Y$, these boundary conditions are identical to those obtained for isotropic media [2]. For the two configurations that we consider, $\epsilon_{XY}^{(2)}=\epsilon_{YX}^{(2)}=\epsilon_{YZ}^{(2)}=\epsilon_{ZY}^{(2)}=0$ and the expression of $\Delta B_X$ becomes $\Delta B_X=-4\pi i(\omega_s/c)P_Y^s$.

By adding to Eq. (A3) the following relations between the components of the field in media 1 and 2:

$$\frac{D_Z^{(1)}}{D_X^{(1)}}=\frac{E_Z^{(1)}}{E_X^{(1)}}=\frac{k_X}{k_Z^{(1)}} ,$$

$$\frac{D_Z^{(2)}}{D_X^{(2)}}=\frac{\epsilon_{ZX}^{(2)}E_X^{(2)}+\epsilon_{ZZ}^{(2)}E_Z^{(2)}}{\epsilon_{XX}^{(2)}E_X^{(2)}+\epsilon_{XZ}^{(2)}E_Z^{(2)}}=-\frac{k_X}{k_Z^{(2)}} , \tag{A4}$$

one can calculate the $p$-component of the field radiated in medium 1 by the polarization sheet:

$$E_p^{(1)}=4\pi ik^{(1)}k_Z^{(1)}\frac{p_Z^s}{k_Z^{(2)}\epsilon_{ZZ}^{(2)}-\epsilon^{(1)}\epsilon_{ZZ}^{(2)}(k_X\epsilon_{XZ}^{(2)}+k_Z^{(2)}\epsilon_{ZZ}^{(2)})(\epsilon_{XZ}^{(2)}\epsilon_{ZX}^{(2)}-\epsilon_{ZZ}^{(2)}\epsilon_{XX}^{(2)})^{-1}}\exp(i\mathbf{k}^{(1)}\cdot\mathbf{r}-i2\omega t) , \tag{A5}$$

where all dielectric constants are at frequency $2\omega$.

In order to calculate $E_p^{(1)}$ numerically for $\Phi_0=0°$ and 180°, we have used the following parameters: $\theta_1=45°$, $\beta=5°$ [24], $n_{ab}(\omega)=1.57, n_c(\omega)=1.53, n_{ab}(2\omega)=1.6$, and $n_c(2\omega)=1.56$ [44]. We find

$$\frac{E_p^{(1)}(\Phi_0=0°)}{E_p^{(1)}(\Phi_0=180°)}=0.96 . \tag{A6}$$

We can thus conclude that $\Phi=0°$ and 180° in Fig. 16 correspond to the beam geometries depicted respectively in Figs. 17(b) and 17(a) with the $X$ axis of the light reference frame being respectively antiparallel and parallel to the vector $\hat{l}$ lying in the glide plane $\Sigma$ of mica defined in Fig. 3.

## APPENDIX B: ORIENTATIONAL DISTRIBUTION OF LIQUID-CRYSTAL MOLECULES IN MONOLAYERS

We compare here the orientational distributions found using the maximum-entropy method [Eq. (7)] with the one obtained in previous work using a specific distribution function [Eq. (4)]. We take as example the case of 8CB ($NC\Phi\Phi C_8H_{17}$) molecules on rubbed polyimide. Using the distribution given in Eq. (4), the authors found $\theta_0=76°$, $\sigma=5°$, $d_1=0.06$, $d_2=0.43$, and $d_3=-0.001$ [4,5], which gives the distribution plotted in Fig. 19(a). Using the maximum-entropy method [Eq. (7)], we find the distribution plotted in Fig. 19(b).

In the latter case (distribution $b$), the distributions in $\theta$ and $\phi$ are nearly independent. This independence is assumed in the former case (distribution $a$) which is *a posteriori* justified. Distribution $a$ exhibits two peaks for ($\theta=76°$, $\phi=0°$) and ($\theta=76°$, $\phi=180°$). Distribution $b$ exhibits three peaks for ($\theta=61°$, $\phi=0°$), ($\theta=59°$, $\phi=180°$), and $\theta=180°$. The proportion of molecules in the latter peak, which is missing in distribution $a$, is approximately 15%. These molecules point with their cyano group away from the substrate surface while the rest of the molecules points with their cyano group towards the surface. The other peaks are located for different tilt angles $\theta$ in the two distributions. In distribution $a$, they are shifted towards higher values of $\theta$. This is caused by the absence of the peak at $\theta=180°$: using the maximum-entropy method with the assumption that all the molecules point with their cyano group towards the surface [$f(\theta,\phi)=0$ for $90°\leq\theta\leq180°$] give a distribution nearly identical to distribution $a$ [Fig. 19(c)].

Generally speaking, the maximum-entropy method gives two possible orientational distributions for the surface liquid-crystal molecules: one in which orientations of the molecules with the cyano group away from the surface are *a priori* forbidden and one in which these orientations are allowed. The latter distribution gives the upper limit of the proportion of molecules pointing with their cyano group away from the surface: as its name indicates, the maximum-entropy method gives the distribution with the maximum spreading over all allowed orientations compatible with the experimental data. The actual distribution is somewhere in between the two limiting distributions just described. In order to choose which of these distributions better approximates the actual distribution, one should use either additional experimental information about the distribution (not available so far) or

estimates of the proportion of molecules pointing with their cyano group away from the surface, which can be obtained by calculating the energy of the different orientations at the surface.

When the ratio $\langle \cos^3\theta \rangle / \langle \cos\theta \rangle$ is found to be negative, the proportion of molecules pointing with their cyano group away from the surface cannot be zero. One can then calculate only one of the limiting distributions. In order to estimate the minimum value this proportion can take, we can consider a simple $\theta$ distribution close to those obtained for liquid-crystal monolayers:

$$\begin{aligned} &f(\theta)=0, \quad 0^\circ \le \theta \le 45^\circ , \\ &f(\theta)=f_1, \quad 45^\circ \le \theta \le 90^\circ , \\ &f(\theta)=0, \quad 90^\circ \le \theta \le 135^\circ , \\ &f(\theta)=f_2, \quad 135^\circ \le \theta \le 180^\circ . \end{aligned} \tag{B1}$$

The minimum proportion of molecules with their cyano group pointing away from the surface leading to a negative ratio $\langle \cos^3\theta \rangle / \langle \cos\theta \rangle$ is obtained for $f_1 = 3f_2$ and is 12%.


[1] B. Jérôme, Rep. Prog. Phys. **54**, 391 (1991).

[2] Y. R. Shen, Nature **337**, 519 (1989); Y. R. Shen, Annu. Rev. Phys. Chem. **40**, 327 (1989).

[3] J. S. Foster and J. E. Frommer, Nature **333**, 542 (1988); D. P. E. Smith, H. Hörber, C. Gerber, and G. Binnig, Science **245**, 43 (1989).

[4] W. Chen, M. Feller, and Y. R. Shen, Phys. Rev. Lett. **63**, 2665 (1989).

[5] M. B. Feller, W. Chen, and Y. R. Shen, Phys. Rev. A **43**, 6778 (1991).

[6] M. Barmentlo, R. W. J. Hollering, and N. A. J. M. van Aerle, Phys. Rev. A **46**, 4490 (1992).

[7] P. Pieranski and B. Jérôme, Mol. Cryst. Liq. Cryst. **199**, 167 (1991).

[8] G. Ryschenkow and M. Kleman, J. Chem. Phys. **64**, 404 (1976).

[9] S. Faetti and L. Fronzoni, Solid State Commun. **25**, 1987 (1978); P. Chiarelli, S. Faetti, and L. Fronzoni, J. Phys. (Paris) **44**, 1061 (1983).

[10] K. Hiltrop and H. Stegemeyer, Ber. Bunsenges. Phys. Chem. **85**, 582 (1981); in *Liquid Crystals and Ordered Fluids, Vol. 4,* edited by A. C. Griffin and J. F. Johnson (Plenum, New York, 1984), p. 515.

[11] G. E. Volovik and O. Lavrentovitch, Zh. Eksp. Teor. Fiz. **85**, 1997 (1983) [Sov. Phys. JETP **58**, 1159 (1984)].

[12] P. Pieranski and B. Jérôme, Phys. Rev. A **40**, 317 (1989).

[13] J. Bechhoefer, J. L. Duvail, L. Masson, B. Jérôme, R. M. Hornreich, and P. Pieranski, Phys. Rev. Lett. **64**, 1911 (1990).

[14] H. S. Kitzerow, B. Jérôme, and P. Pieranski, Physica A **174**, 163 (1991).

[15] W. M. Gibbons, P. J. Shannon, S. T. Sun, and B. J. Swetlin, Nature **351**, 49 (1991).

[16] K. Flatisher, L. Komitov, S. T. Lagerwall, B. Stebler, and A. Strigazzi, Mol. Cryst. Liq. Cryst. **198**, 119 (1991).

[17] M. Petrov, A. Braslau, A. M. Levelut, and G. Durand, J. Phys. (Paris) II **2**, 1159 (1992).

[18] A. G. Dyadyusha, T. Ya. Marusiĭ, Yu. A. Reznikov, A. I. Khizhnyak, and V. Yu. Reshetnyak, Pis'ma Zh. Eksp. Teor. Fiz. **56**, 18 (1992) [JETP Lett. **56**, 17 (1992)].

[19] J. S. Patel and H. Yokoyama, Nature **362**, 525 (1993).

[20] B. Jérôme, J. O'Brien, Y. Ouchi, C. Stanners, and Y. R. Shen, Phys. Rev. Lett. **71**, 758 (1993).

[21] P. Pieranski, B. Jérôme, and M. Gabay, Mol. Cryst. Liq. Cryst. **179**, 285 (1990).

[22] P. I. C. Teixeira and T. J. Sluckin, J. Chem. Phys. **97**, 1498 (1992); **97**, 1510 (1992).

[23] T. F. Heinz, in *Nonlinear Surface Electromagnetic Phenomena,* edited by H. E. Ponath and G. I. Stegeman (Elsevier, Amsterdam, 1991), p. 353.

[24] Micas, Vol. 13 of *Reviews of Mineralogy,* edited by S. W. Bailey (Brookcrafters, Chelsea, 1987).

[25] A. J. Leadbetter, J. P. Frost, J. C. Gaughan, C. W. Gray, and A. Mosley, J. Phys. (Paris) **40**, 375 (1979).

[26] H. Hsiung and Y. R. Shen, Phys. Rev. A **34**, 4303 (1986).

[27] P. Guyot-Sionnest, H. Hsiung, and Y. R. Shen, Phys. Rev. Lett. **57**, 2963 (1986).

[28] G. Berkovic, Physica A **168**, 140 (1990).

[29] P. Guyot-Sionnest, W. Chen, and Y. R. Shen, Phys. Rev. B **33**, 8254 (1986); P. Guyot-Sionnest and Y. R. Shen, *ibid.* **38**, 7985 (1988).

[30] In the whole article, it should be kept in mind that when we use for simplicity the words "molecular axis" and "molecular orientation," we actually speak of the axis and the orientation of the rigid cyanobiphenyl core of the liquid-crystal molecules and not those of the whole molecules; the rigid core is the only part of the molecules having a significant nonlinear polarizability and is thus the only part whose orientation can be probed by second-harmonic-generation measurements.

[31] B. Jérôme and P. Pieranski, Europhys. Lett. **13**, 55 (1990).

[32] The $C_s$ symmetry of the mica surface is in fact slightly broken [31]. We have tried to analyze our data assuming a $C_1$ surface symmetry, but the data turned out not to be precise enough to allow us to determine the four additional nonzero components of $\overline{\chi}^D$ existing in this case.

[33] J. Bechhoefer, B. Jérôme, and P. Pieranski, Phys. Rev. A **41**, 3187 (1990).

[34] C. S. Mullin, P. Guyot-Sionnest, and Y. R. Shen, Phys. Rev. A **39**, 3745 (1989).

[35] In fact, the organization of the liquid-crystal molecules in bilayers (which can occur close to the surface [37]) quickly decays away from the substrate surface since there is no positional order in bulk nematic liquid crystals. It is nevertheless convenient to assume this organization in the whole film in order to estimate its thickness.

[36] The upper layer in contact with air does not exhibit any polar ordering [26].

[37] J. Als-Nielsen, F. Christensen, and P. S. Pershan, Phys. Rev. Lett. **48**, 1107 (1982).

[38] E. T. Jayne, Phys. Rev. **106**, 620 (1957).

[39] Y. Ouchi, M. B. Feller, T. Moses, and Y. R. Shen, Phys. Rev. Lett. **68**, 3040 (1992).

[40] W. Maier and A. Z. Saupe, Z. Naturforsch. A **13**, 564 (1958).

[41] J. H. Hunt, P. Guyot-Sionnest, and Y. R. Shen, in *Laser*

*Spectroscopy,* edited by W. Persson and S. H. Svanberg (Springer-Verlag, Berlin, 1987), p. 253.
[42] K. J. Laidler, *Principles of Chemistry* (Harcourt, Brace & World, New York, 1966).
[43] A. J. van der Est, M. Y. Kok, and E. E. Burnell, Mol. Phys. **60**, 397 (1987); D. S. Zimmerman and E. E. Burnell, *ibid.* **69**, 1059 (1990).
[44] The refractive index $n_{ab}(\omega)$ of our mica sample for $\omega=2\pi/532$ nm$^{-1}$ has been measured by M. Rubin from the Lawrence Berkeley Laboratories. $n_{ab}(2\omega)$ was estimated to be close to $n_{ab}(\omega)$ from the fact that the reflectivity is the same at these two frequencies. $n_c(\omega)$ and $n_c(2\omega)$ have been calculated from the known birefringence [24], which is assumed to be the same at frequencies $\omega$ and $2\omega$.